Signature of Arctic surface ozone depletion events in the isotope anomaly ($\Delta 17O$) of atmospheric nitrate

S. Morin, J. Savarino, Slimane Bekki, S. Gong, J. W. Bottenheim

Atmos. Chem. Phys., 7, 1451–1469, 2007
www.atmos-chem-phys.net/7/1451/2007/

Atmospheric Chemistry and Physics

Signature of Arctic surface ozone depletion events in the isotope anomaly (Δ^{17}O) of atmospheric nitrate

S. Morin[1], **J. Savarino**[1], **S. Bekki**[2], **S. Gong**[3], **and J. W. Bottenheim**[3]

[1]Laboratoire de Glaciologie et de Géophysique de l'Environnement, Centre National de la Recherche Scientifique – Université Joseph Fourier, Grenoble, France
[2]Service d'Aéronomie, Institut Pierre Simon Laplace, Université Pierre-et-Marie Curie, Paris, France
[3]Environment Canada, Toronto, Ontario, Canada

Received: 21 April 2006 – Published in Atmos. Chem. Phys. Discuss.: 12 July 2006
Revised: 12 February 2006 – Accepted: 6 March 2007 – Published: 13 March 2007

Abstract. We report the first measurements of the oxygen isotope anomaly of atmospheric inorganic nitrate from the Arctic. Nitrate samples and complementary data were collected at Alert, Nunavut, Canada (82°30′ N, 62°19′ W) in spring 2004. Covering the polar sunrise period, characterized by the occurrence of severe boundary layer ozone depletion events (ODEs), our data show a significant correlation between the variations of atmospheric ozone (O_3) mixing ratios and Δ^{17}O of nitrate ($\Delta^{17}O(NO_3^-)$). This relationship can be expressed as: $\Delta^{17}O(NO_3^-)/‰ = (0.15\pm0.03)\times O_3/(\text{nmol mol}^{-1})+(29.7\pm0.7)$, with R^2=0.70(n=12), for $\Delta^{17}O(NO_3^-)$ ranging between 29 and 35 ‰.

We derive mass-balance equations from chemical reactions operating in the Arctic boundary layer, that describe the evolution of $\Delta^{17}O(NO_3^-)$ as a function of the concentrations of reactive species and their isotopic characteristics. Changes in the relative importance of O_3, RO_2 and BrO in the oxidation of NO during ODEs, and the large isotope anomalies of O_3 and BrO, are the driving force for the variability in the measured $\Delta^{17}O(NO_3^-)$. $BrONO_2$ hydrolysis is found to be a dominant source of nitrate in the Arctic boundary layer, in agreement with recent modeling studies.

1 Introduction

Stable isotope studies have been used since the 1930s to constrain fluxes and processes taking place at the surface of the Earth. Mass-dependent processes such as thermodynamic equilibria lead to a quasi-linear relationship between oxygen isotope ratios in oxygen bearing compounds: $\delta^{17}O\simeq0.52\delta^{18}O$, with the isotopic content reported as enrichments with respect to a reference material: $\delta=(R_{sample}/R_{SMOW}-1)$ where R is the $^{17}O/^{16}O$ or $^{18}O/^{16}O$ ratio in the sample or the Standard Mean Ocean Water (SMOW) taken as a reference (Baertschi, 1976; Li et al., 1988).

Thiemens and Heidenreich III (1983) discovered that mass-independent fractionation (MIF) occurred when ozone was produced from molecular oxygen. The resulting isotope anomaly measured in atmospheric ozone (Krankowsky et al., 1995; Johnston and Thiemens, 1997; Mauersberger et al., 2001) can be quantified as a deviation from the mass-dependent fractionation line as follows: $\Delta^{17}O=\delta^{17}O-0.52\times\delta^{18}O$. The isotope anomaly of ozone is transmitted through chemical reactions in the atmosphere to other oxygen bearing compounds (Thiemens, 2006). Michalski et al. (2003) showed that simple kinetics box-modeling could reproduce the temporal evolution of the isotope anomaly measured in particulate nitrate in a polluted marine boundary layer. Here we present the coupled evolution of $\Delta^{17}O(NO_3^-)$ and ozone mixing ratio at Alert, Nunavut (82°30′ N, 62°19′ W) during the polar sunrise period in spring 2004. At Alert, like everywhere else in the coastal Arctic, surface ozone is subject to severe depletion events (ODEs) in springtime (Bottenheim et al., 1986), during which the ozone mixing ratio can decrease from around 40 parts-per-billion in volume (nmol mol^{-1}), its mean background level, to values below the detection limit, and remain at this level for several hours to several days (Bottenheim et al., 2002). Ozone depletion is due to catalytic cycles involving ocean-originating halogen oxides and radicals such as BrO (Hönninger and Platt, 2002) but the understanding of the processes governing the release of such compounds from the surface is still a subject of debate (Domine and Shepson, 2002).

To the best of our knowledge, we report the first measurements of Δ^{17}O of atmospheric nitrate in the coastal Arctic, thereby expanding the global coverage of measurements of this variable. Permanent sunshine, sea-ice proximity and the associated halogen chemistry responsible for ODEs call

Correspondence to: S. Morin)
(samuel.morin@lgge.obs.ujf-grenoble.fr

Published by Copernicus GmbH on behalf of the European Geosciences Union.

for a detailed assessment of the mechanisms leading to the production of atmospheric nitrate in these peculiar environmental conditions, in order to interpret the variations in the $\Delta^{17}O(NO_3^-)$ record.

2 Experimental

2.1 Measurement site and sample collection

Measurements and sample collection were performed at the Global Atmospheric Watch (GAW) observatory and at the Special Studies Trailer (SST) which are located on a plateau, 190 m above sea level and 6 km to the south-southwest of Canadian Forces Station Alert, the main base at the coast of Northern Ellesmere Island, from 29 March 2004 until 18 May 2004.

Surface ozone was measured at the SST site with a UV absorption instrument (model TEI 49-C, Thermo Environmental Instruments, Inc., Franklin MA, USA), calibrated against standards traceable to the National Institute of Standards and Technology (NIST). Measurements with this instrument were terminated on 4 May 2004. In order to analyze ozone measurements during the entire period of isotopic measurements, the gap between 4 and 18 May 2004 was filled by using the raw (uncalibrated) ozone GAW dataset, and recalibrating using a linear regression against the SST ozone dataset over the overlapping period of measurements. The time resolution for ozone measurements is 30 min.

Aerosol samples were collected on cellulose acetate filters (Whatman 41) on a semi-weekly basis using a high volume aerosol sampler operated by Environment Canada since 1980 (see e.g. Sirois and Barrie (1999) for details on sampling procedures). Each of the 14 samples was collected over a period of 3 or 4 days.

2.2 Chemical composition analysis

First, ionic species trapped on the filter were dissolved in 40 ml of ultra-pure water (Millipore). 100 μl aliquots were analyzed for major anions (Cl^-, Br^-, NO_3^- and SO_4^{2-}) and cations (Na^+, Ca^{2+}, Mg^{2+}, K^+ and NH_4^+) using the ion-chromatography system described in Jaffrezo et al. (1998). Four field blanks were performed to assess the contribution of possible contaminations induced by the manipulation of filters and by the filters themselves because Whatman 41 filters were questioned regarding their initial content in some trace elements (Watts et al., 1987). Field blank samples were obtained by loading clean filters in the sampler, keeping them there for 5 min and packing them exactly like the actual samples. The contamination term was estimated by dividing the measured amount of species by the typical volume pumped through regular filters (ca. 10 000 m^3).

For the samples presented here, the blank contribution, integrating all possible sources of contaminations, represents less than 4% for all the measured cations. The contribution of contamination to the total measured NO_3^-, SO_4^{2-} and Br^- is less than 1%. Only Cl^- measurements are affected by a 10% blank effect. The collection efficiency of this sampling device has been estimated to be >95% by Sirois and Barrie (1999), based on previous work by Watts et al. (1987).

Existing literature on the collection of atmospheric inorganic nitrate by means of high volume sampling on a variety of media show that none is devoid of sampling artefact (e.g. Schaap et al., 2002). The use of cellulose acetate filters leads to the quantitative collection of both particulate nitrate ($p-NO_3^-$, in the form of ammonium nitrate and other nitrate salts) and gaseous nitric acid (HNO_3), the sum of which being referred to as total inorganic nitrate (TIN, Bottenheim et al., 1993). However, it is worth keeping in mind that the measurements of $\Delta^{17}O(NO_3^-)$ based on filter collection are not suspected to be sensitive to the chemical form of nitrate (either gaseous HNO_3 or particulate NO_3^-) because any fractionation occurring at the interface between the gas phase and the particulate phase obeys mass-dependent relationships, without affecting the $\Delta^{17}O$ value. In what follows, we present and discuss $\Delta^{17}O(NO_3^-)$ measurements, which represent the integrated isotope anomaly of oxygen of TIN.

2.3 Isotopic analysis

The isotopic analysis was performed using the method developed by Michalski et al. (2002). Chloride and sulphate were precipitated out of the samples, using $BaCl_2$ for SO_4^{2-} and subsequent removal of chloride using an Ag-form ion-exchange resin (AG 50W-X8 200-400 Mesh size, Bio-Rad, Hercules CA, USA). Nitrate was then isolated by Dionex ion chromatography and converted to silver nitrate using an ion exchange column (Dionex AMMS III, 4 mm) where the usual regenerant was replaced by Ag_2SO_4 (2.5 mmol l^{-1}). The triple isotope composition of oxygen in $AgNO_3$ was determined by thermal decomposition at 550°C in a vacuum line and analysis on an isotope ratio mass-spectrometer (Dual Inlet IRMS, Finnigan MAT 253). All the analytical steps were simultaneously performed on nitrate standards (International Atomic Energy Agency USGS 34 and USGS 35, with $\Delta^{17}O$=-0.1 ‰ for USGS 34 and 21.6 ‰ for USGS 35, Böhlke et al., 2003). A correction of the raw $\Delta^{17}O$ values was performed in order to remove the effect of the contamination from the formation of silver oxide at the surface of the silver capsules used for the thermal decomposition of $AgNO_3$ (Michalski et al., 2002). This contamination was estimated to be on the order of (0.16±0.05) µmol of ambient O_2 ($\Delta^{17}O(O_2)$=-0.3 ‰, Barkan and Luz, 2005), to be compared with the size range of our samples (between 1 and 2 µmol of O_2 after the decomposition). A mass balance equation was used to correct each measured value for this contamination effect.

Uncertainties on the $\Delta^{17}O(NO_3^-)$ values originate from the internal reproducibility of the mass spectrometer

(accounting for about ±0.3 ‰ for a detector voltage of 500 mV in average) and from the correction of the blank effect (accounting for about ±1.0 ‰, due to the propagation of the uncertainty affecting the size of the contamination term, see above). Both of these sources of uncertainty vary with the size of the samples. Because of an extremely low concentration of nitrate in two samples, the thermal decomposition yielded a too small amount of O_2 to be reliably analyzed. Therefore we present here the data obtained on 12 samples in terms of their isotopic composition.

All $\Delta^{17}O$ values reported in this article were calculated from the $\delta^{17}O$ and $\delta^{18}O$ values using the linear expression:

$$\Delta^{17}O = \delta^{17}O - \lambda \times \delta^{18}O (\lambda = 0.52) \quad (1)$$

This definition for $\Delta^{17}O$ has been extensively used for nitrate oxygen isotopes (Michalski et al., 2002, 2003; Alexander et al., 2004; McCabe et al., 2005; Savarino et al., 2006). It has the advantage over alternative forms (e.g. Miller, 2002; Böhlke et al., 2003; Kaiser et al., 2004; Zahn et al., 2006) that mass-balance calculations can algebraically be easily derived (Kaiser et al., 2004). In addition, for nitrate, generally characterized by elevated (>20 ‰) isotope anomalies in atmospheric contexts, the choice for the mathematical expression of $\Delta^{17}O$ is not as crucial as for slightly anomalous species (e.g. N_2O), for which the linear definition may be responsible for inaccuracies and interpretation errors, as pointed out by Kaiser et al. (2004). The difference between $\Delta^{17}O$ values calculated with two different definitions generally lies within less than 1 ‰ for atmospheric nitrate samples.

3 Results

We present the data acquired in Alert, Nunavut, between 29 March 2004 and 18 May 2004. They mainly consist of meteorological observations (temperature and precipitations), ozone mixing ratios, aerosol inorganic composition and the triple isotopic composition of oxygen in inorganic nitrate.

3.1 Meteorology

During the course of the measurement campaign, sunlight was permanent. The mean daily temperature ranged between −30 and −10°C, gradually increasing over the measurement campaign. Cumulative precipitation (snow) was 22 mm during this period, with only one major (>8 mm) snowfall occurring on 12 April 2004. Weather conditions were most of the time calm and clear. The barometric pressure ranged between 999 and 1042 hPa over the course of the measurement campaign.

3.2 Ozone

The ozone mixing ratio was highly variable during this period, and its time series features several drastic drops, commonly referred to as ozone depletion events (ODEs) which

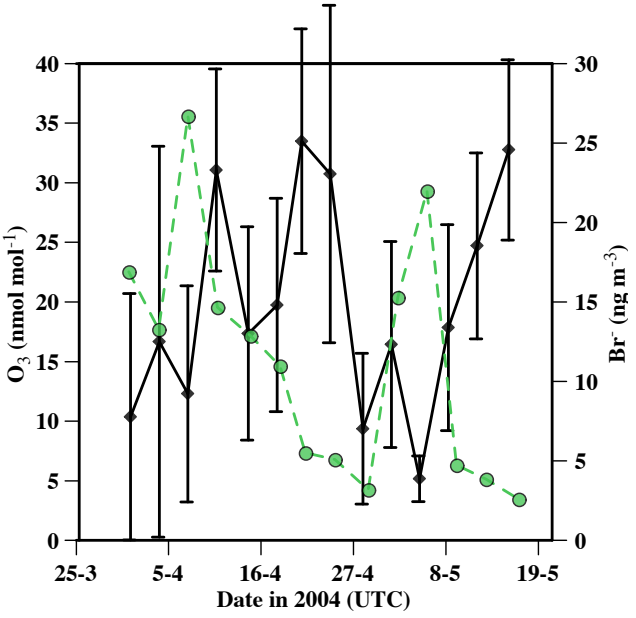

Fig. 1. Time series of the ozone mixing ratio (diamonds, black line) and particulate bromide concentration (circles, green dashed line). The error bars associated to the ozone mixing ratio represent its variability (1σ) within each averaging period. The concentration of particulate bromide carries an uncertainty of about 10%, not shown for clarity.

are ubiquitously observed in coastal polar regions (see the high-resolution time series on Fig. 3) (Tarasick and Bottenheim, 2002). To quantify its link with the other variables, the ozone mixing ratio was averaged over each sampling period (i.e. 3–4 days). The minimum averaged ozone mixing ratio was (5.2±1.9) nmol mol^{-1}.

3.3 Particulate bromide and BrO

The Fig. 1 shows the coupled evolution of the ozone mixing ratio and the particulate bromide content. Particulate bromide (Br^-) ranged between 2 and 20 ng m^{-3}. Elevated Br^- levels (>10 ng m^{-3}) were associated in two cases with ozone depleted air masses, which is consistent with the first observations at Alert (Barrie et al., 1988). Particulate bromide originates from the conversion of BrO_x (≡ Br + BrO) and is indicative of the intensity of the halogen-mediated ODE chemistry. However, as evidenced by Lehrer et al. (1997) and Evans et al. (2003), inferring BrO mixing ratio from Br^- is only possible for limited periods of times.

Unfortunately no continuous record of BrO is currently available for the spring 2004 period at Alert, but on some occurrences the mixing ratio of BrO could be derived from Multi-Axis Differential Optical Absorption Spectroscopy (MAX-DOAS) measurements carried out at Alert or in its vicinity. Morin et al. (2005) have shown that on 22–23 April 2004, BrO ranged between 1–3 pmol mol^{-1} ("normal"

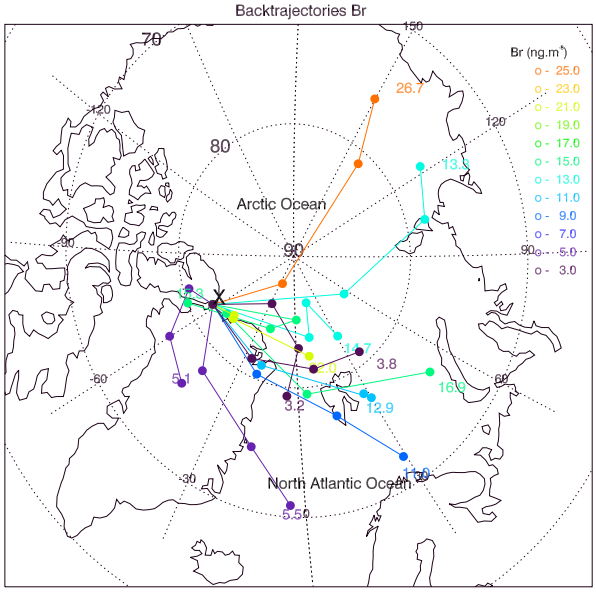

Fig. 2. Mean 6-days backtrajectories of air masses arriving at Alert during the sampling period (March–April 2004). Each backtrajectory is a mean of all the backtrajectories starting from Alert every 6 h during the collection period (about 3–4 days) of each aerosol sample (for a total of 12 samples). This provides an indication of the origin and history of air masses contributing to a given aerosol sample. The filled circles represent the position of the air masses every 2 days. The circles and lines are color-coded according to the particle bromide concentration measured in each sample (in ng m^{-3}). Note that most samples with enhanced bromide concentration are associated with trajectories originating from the Siberian side of the Arctic basin or to rather motionless air masses, sitting over the Arctic Ocean. Such areas are believed to be key locations for the bromine heterogeneous chemistry involved in Arctic surface ozone depletion events.

ozone) and 10 pmol mol^{-1} (strong ODE). This is in line with measurements presented by Hönninger et al. (2004), carried out in the vicinity of Alert in spring 2004. Overall, there seems to be evidence that, even during the strongest ODEs, BrO never reached values significantly above 10 pmol mol^{-1} in spring 2004.

Moreover, we could make use of the inverse correlation between the mixing ratios of BrO and ozone, presented by Hönninger and Platt (2002). However, the data obtained by Hönninger and Platt (2002) at Alert show that BrO levels rise over 5 pmol mol^{-1} only when ozone mixing ratios drop below the threshold of 5 nmol mol^{-1}. For moderate levels of ozone (> 5 nmol mol^{-1}), the mixing ratio of BrO is more or less constant and fluctuates around 2 pmol mol^{-1}.

3.4 Origin of air masses

Following the approach of Bottenheim and Chan (2006) and previous trajectory studies, 6-days backtrajectories (Stohl et al., 1995; Stohl and Seibert, 1998; Stohl, 1998) starting at Alert during the sampling period (March–April 2004) were used to identify the origin and history of air masses. The meteorological data used for trajectory calculations originates from the European Centre for Medium Range Weather Forcasts (ECMWF). The spatial resolution is T106, which corresponds to a latitude/longitude resolution of 1.125°×1.125°, the temporal resolution is 6 h and 60 levels are available in the vertical direction. It is worth pointing out that trajectories for surface sites calculated from large-scale meteorological analyses are certainly far from being very accurate. Although their usefulness is limited for specific and small-scale events, they can nonetheless provide relevant information on the gross features when large numbers of trajectories are considered. Each backtrajectory represented in Fig. 2 is a mean of all the backtrajectories starting from Alert at 500 m altitude every 6 h during the collection period (about 3–4 days) of each sample. The method to calculate the mean of N backtrajectories is the following: each mean position is calculated as the mean of the N positions, i.e mean of N longitude and latitude. Note that the mean calculated here using polar coordinates is not the actual mean in a cartesian grid, but this does not have major repercussions in this case because the spread of trajectories for any given sample is small. The trajectories calculated here provide an indication of the mean origin and history of air masses contributing to a given aerosol sample. Backtrajectories starting at 1 km altitude (not shown here) were also considered but the overall features were similar. Each mean trajectory (corresponding to an aerosol sample) is color-coded in Fig. 2 according to its particulate bromide content, which is indicative of the activity of the heterogeneous bromine chemistry responsible for ODEs.

The conclusions that can be drawn from the analysis of the Fig. 2 are in line with other studies discussing the origin of ozone depleted air masses (e.g. Hopper et al., 1998; Morin et al., 2005; Zeng et al., 2006; Bottenheim and Chan, 2006, and references therein). In most cases, drastic changes in the ozone mixing ratios observed at Alert at polar sunrise are related to the movement of air masses. During the course of our measurement campaign, most air masses depleted in ozone were advected at low altitude above the ice pack over the Arctic Ocean region before reaching the coastal sites.

3.5 Inorganic chemical composition of the samples

Our main focus being the analysis of the isotopic composition of TIN, we only present here a summary of our measurements of inorganic chemical composition of aerosols. Extensive reviews of the composition of inorganic aerosols observed at Alert can be found elsewhere (e.g. Sirois and Barrie, 1999).

The relative composition of aerosol in terms of inorganic anions was found to be invariant with time during April and May, but the total amount varied strongly. NO_3^-+SO_4^{2-}+Cl^- ranges between 145 and 1900 ng m^{-3}, in which Cl^-, NO_3^- and SO_4^{2-} represent (7±6)%, (23±8)% and (69±8)% of the

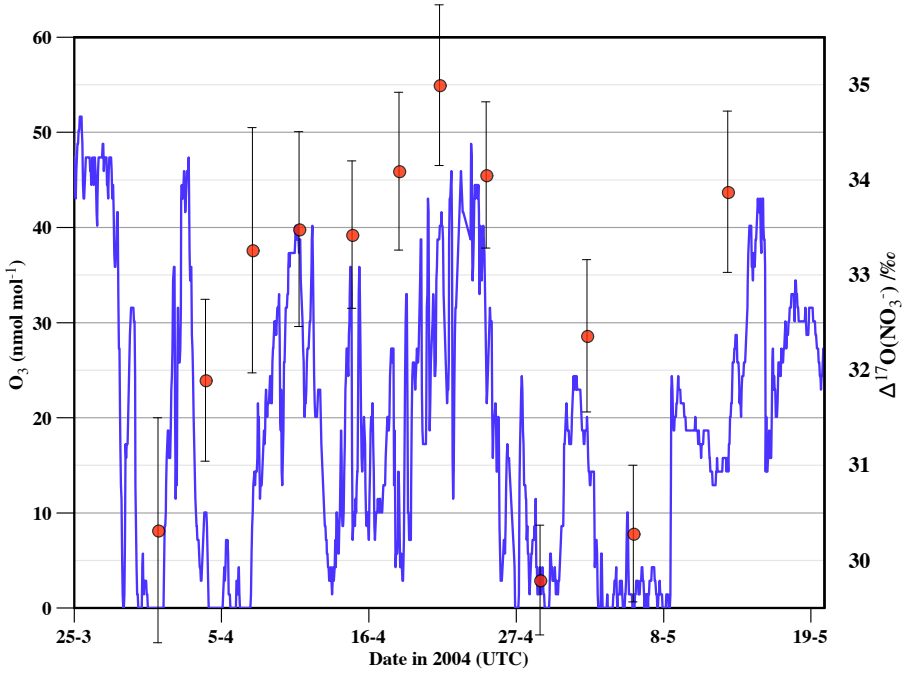

Fig. 3. Coupled evolution of surface O_3 mixing ratio (plain line) and $\Delta^{17}O(NO_3^-)$ (•). Error bars represent the uncertainty due to the mass-spectrometer internal standard error and the correction of the blank effect.

molar composition, respectively. Using a molar $Na^+ : SO_4^{2-}$ ratio in sea salt of 0.0603 (Holland, 1978), the calculated non-sea salt sulphate component (nss$-SO_4^{2-}$) is found to account for more than 99% of the sulphate concentration. Aerosols collected during this study represent a mixture of sulphuric acid droplets and sea salt particles, on which inorganic nitrate is adsorbed (Sirois and Barrie, 1999).

We see no noticeable correlation between the concentration of inorganic nitrate and the origin of air masses (data not shown). Based on nitrate concentrations only, it is virtually impossible to estimate the different sources of particulate nitrate, because alkylnitrate, peroxyalkylnitrates (PANs) and other organic nitrate dominate the budget of nitrate in the Arctic. Thus, the variability in particulate nitrate concentrations does not provide any insight into the budget of nitrate (Sirois and Barrie, 1999).

3.6 Triple isotope composition of oxygen in atmospheric inorganic nitrate

In Table 1, we report elevated ^{18}O enrichments, with $\delta^{18}O$ values ranging from 78 to 92‰. $\Delta^{17}O(NO_3^-)$ ranges between 29 and 35‰ with an average value of 32.7‰ (±1.8‰, one standard deviation). The large temporal variability of $\Delta^{17}O(NO_3^-)$ during this period is shown in Fig. 3. High isotopic enrichments and anomalies are expected in atmospheric nitrate: in terms of range, our measurements are consistent with previous measurements of $\delta^{18}O$ and $\Delta^{17}O$, such as those carried out by Michalski et al. (2003) (La Jolla, California: $\delta^{18}O(NO_3^-)$=50–89‰ and $\Delta^{17}O(NO_3^-)$=20–31‰ during a year-round sampling campaign). More recently, Savarino et al. (2006) reported a year-round survey of atmospheric nitrate isotopes in coastal Antarctica. $\delta^{18}O(NO_3^-)$ values range between 62 and 110‰ and $\Delta^{17}O(NO_3^-)$ values range between 16 and 41‰. High $\delta^{18}O(NO_3^-)$ values were also reported in snow at high latitudes in the northern hemisphere. For example, Hastings et al. (2004) reported $\delta^{18}O(NO_3^-)$ values ranging between 65 and 80‰ in samples collected at Summit, Greenland. Heaton et al. (2004) also found high $\delta^{18}O(NO_3^-)$ values (60–85‰) in samples collected at Ny Ålesund, Svalbard. Finally, Alexander et al. (2004) measured $\Delta^{17}O(NO_3^-)$ in the Site A ice core in Greenland, with values ranging between 27 and 29‰. A direct comparison of our dataset with that of Savarino et al. (2006) is impossible because stratospheric influences interfere with the composition of samples collected in spring in Antarctica, contrary to what is observed in the Arctic. In a polluted marine boundary layer, Michalski et al. (2003) have measured $\Delta^{17}O(NO_3^-)$=23–25‰ in March–May. Our measurements for the same period of the year are significantly higher (+ 9‰ in average, Fig. 6) and strongly variable, with variations as large as 5‰ from one sample to the other. Most of these variations are associated with the occurrence of ODEs. A linear regression between $\Delta^{17}O(NO_3^-)$ and the average ozone mixing ratio over the collection period of each aerosol sample gives: $\Delta^{17}O(NO_3^-)/‰ = (0.15\pm0.03) \times O_3/(\text{nmol mol}^{-1}) +$

Table 1. Summary of the data used in this study. Date ON represents the time (UTC) when the sample started to be collected. Less than 5 min separate each sampling period (data not shown), so the end of sampling corresponds to the beginning of the next sample. All data represent averages over each sampling period.

Date ON UTC (in 2004)	Temp. (1σ) K	NO_3^- ng m^{-3}	O_3 (1σ) nmol mol^{-1}	$\Delta^{17}O(NO_3^-)$ ‰	$\delta^{18}O(NO_3^-)$ ‰
29 March 18:26	243 (5)	52	10.4 (10.3)	30.3 ± 1.2	90 ± 4
1 April 18:26	245 (3)	106	16.7 (16.4)	31.9 ± 0.9	83 ± 4
5 April 19:48	243 (2)	120	12.3 (9.1)	33.3 ± 1.3	85 ± 4
8 April 18:44	244 (4)	150	31.1 (8.5)	33.5 ± 1.0	85 ± 4
12 April 19:40	252 (2)	151	17.4 (9.0)	33.4 ± 0.8	89 ± 4
16 April 15:55	252 (2)	136	19.7 (9.0)	34.1± 0.8	88 ± 4
19 April 20:04	253 (3)	132	33.5 (9.4)	35.0 ± 0.8	88 ± 4
22 April 17:30	257 (4)	142	30.7 (14.2)	34.0 ± 0.8	87 ± 4
26 April 19:16	252 (2)	32	9.4 (6.3)	29.8 ± 0.6	82 ± 4
30 April 17:58	253 (2)	155	16.4 (8.6)	32.4 ± 0.8	84 ± 4
3 May 19:58	253 (2)	110	5.2 (1.9)	30.3 ± 0.7	78 ± 4
7 May 15:19	258 (2)	49	17.8 (8.6)	n.a.	n.a.
10 May 21:18	261 (3)	105	24.7 (7.8)	33.9 ± 0.9	92 ± 4
14 May 17:00	263 (1)	42	32.8 (7.6)	n.a.	n.a.

(29.7±0.7), with R^2=0.70 (n=12), showing that a strong link exists between these two variables (see Fig. 4).

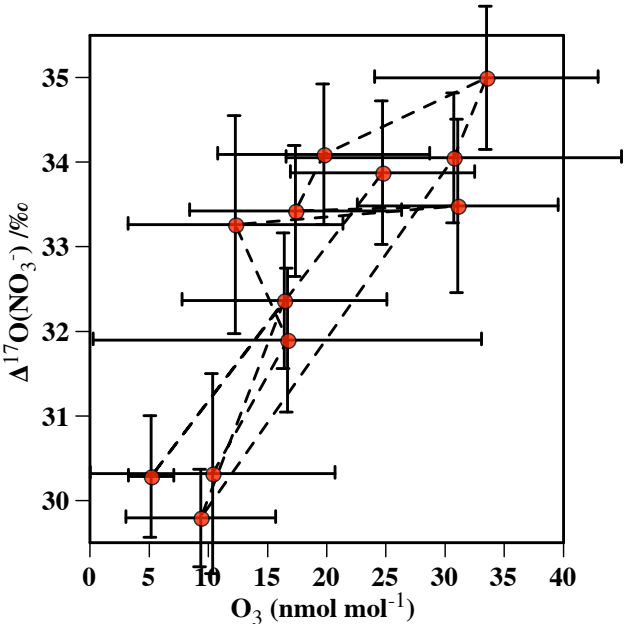

Fig. 4. Correlation plot of $\Delta^{17}O(NO_3^-)$ vs. O_3. Ozone measurements are averaged over the collection period of each aerosol sample, horizontal error bars refer to one standard deviation. The linear regression is: $\Delta^{17}O(NO_3^-)$/‰=(0.15±0.03) $\times O_3$ /(nmol mol^{-1})+(29.7±0.7), with R^2=0.70 (n=12). The dash line indicates the chronological order.

4 Ozone, nitrogen oxides and bromine oxides chemistry in the springtime Arctic troposphere

The isotope anomaly of ozone is transferred to the precursors of nitrate in various proportions depending on the reaction pathway. Identifying and quantifying the relative magnitude of each of them, and their possible variations, are key towards understanding the origin for the isotope anomaly measured in TIN and its temporal variations (Michalski et al., 2003). First of all, we briefly recall the basic tropospheric chemistry of ozone and nitrogen oxides, and classical pathways leading to the formation of nitrate. Then, we detail the key processes responsible for the depletion of ozone in the Arctic troposphere. Finally, we show how ODE-related processes could affect the budget of nitrogen oxides and the formation of nitrate.

4.1 Basic tropospheric chemistry of ozone and nitrogen oxides

In most of the troposphere, nitrate is known to be formed from the oxidation of nitrogen oxides (e.g. Finlayson-Pitts and Pitts, 2000):

– nitrogen oxides (NO_x) are primarily recycled through the following photochemical cycle :

$$NO_2 \xrightarrow{h\nu} NO + O(^3P)\ J \quad \text{(R1)}$$

$$O(^3P) + O_2 \xrightarrow{M} O_3 \quad k_{O+O_2} \quad \text{(R2)}$$

$$NO + O_3 \rightarrow NO_2 + O_2 \quad k_{NO+O_3} \quad \text{(R3)}$$

$$NO + RO_2 \rightarrow NO_2 + RO \quad k_{NO+RO_2} \quad \text{(R4)}$$

where RO_2 represents all peroxy and alkyl-peroxy radicals.

– NO_2 is converted into atmospheric nitric acid and particulate nitrate through one of the following main reaction pathways :

$$NO_2 + OH \xrightarrow{M} HNO_3 \quad \text{(R5)}$$

$$NO_2 + O_3 \rightarrow NO_3 + O_2 \quad \text{(R6)}$$

$$NO_3 + RH \rightarrow HNO_3 + \text{products} \quad \text{(R7)}$$

$$NO_3 + NO_2 \rightleftharpoons N_2O_5 \xrightarrow{H_2O} 2HNO_3 \quad \text{(R8)}$$

The recycling of nitrogen oxides occur on time scales of minutes (lifetime of NO_2 with respect to photolysis) and the conversion into nitric acid occurs on time scales of a day typically.

4.2 Bromine oxide (BrO_x) chemistry and ozone depletion events

It is now well established that bromine is the key radical responsible for tropospheric ozone depletion in the Arctic (Bottenheim et al., 2002). Bromine originates from sea-salt. The exact location where bromide is activated into radical forms, that can destroy ozone, is still a subject of intense research (Domine and Shepson, 2002; Sander et al., 2006).

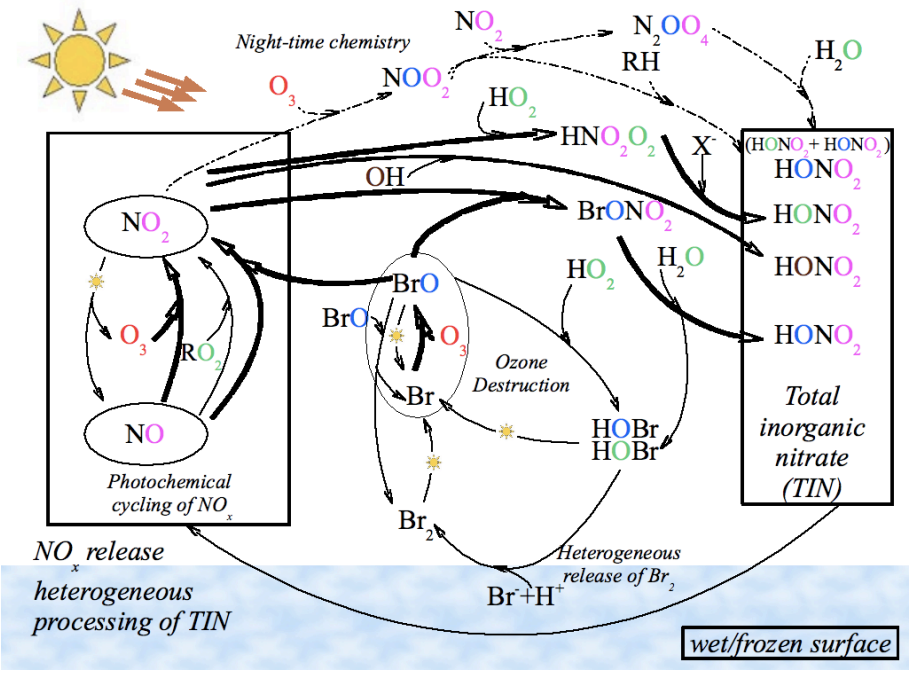

Fig. 5. Chemical cycling of nitrogen oxides (NO_x) and total inorganic nitrate (TIN) in the context of ODEs in the Arctic spring at Alert. Oxygen atoms are color coded according to their isotope anomaly, determined by the reaction between parent molecules (red : $\Delta^{17}O$ of ozone (25–35 ‰), green : $\Delta^{17}O$ = 0 ‰, braun : $\Delta^{17}O$(OH) (variable), blue : $\Delta^{17}O$ of terminal oxygen atoms of ozone (30–42 ‰), violet : $\Delta^{17}O$ of NO_2 (variable, see text for details)). The night-time chemistry channels are mentioned for completeness (2 dots 3 dashes-arrows). Note that these channels are suppressed in the case of this study, since sunlight was permanent during the sampling campaign. Major reactions involved in anomalous oxygen transfer (for day-light reactions only) are highlighted using thicker arrow. Processes responsible for the release and the cycling of BrO are simplified (modified after Hönninger and Bottenheim, 2003).

Sea-salt aerosols (Fan and Jacob, 1992), but also the seasonal snowpack (Tang and McConnell, 1996; Sander et al., 1997; Michalowski et al., 2000) should be the predominant sources of bromine in the atmosphere.

BrO is produced by reaction of Br with ozone, and plays an important role in the ozone destruction catalytic cycle (Platt and Hönninger, 2003):

$$Br + O_3 \rightarrow BrO + O_2 \quad \text{(R9)}$$

BrO can either self-react to return Br_2 and O_2, or react with HO_2 to form HOBr and O_2. Both Br_2 and HOBr are photolabile, so that they are easily photolyzed into Br and OH. In acidic conditions, HOBr may also activate condensed-phase bromide through the reaction :

$$HOBr + Br^- + H^+ \rightarrow Br_2 + H_2O \quad \text{(R10)}$$

The catalytic cycles of BrO_x in both the gas phase and the condensed phase are responsible for the so-called "bromine explosion" (Platt and Janssen, 1996) which results in a fast and efficient removal of ozone within the Arctic boundary layer. In these conditions, elevated levels of BrO were measured (Hönninger and Platt, 2002), with peak values as high as 30 pmol mol^{-1} during a strong ODE near Alert in spring 2000.

In what follows, we neglect Cl chemistry, since Br is by far the most active halogen during ODEs (Hönninger and Platt, 2002). However, taking into account Cl would be crucial for stratospheric studies where chlorine chemistry dominates over bromine chemistry.

4.3 $HO_x-NO_x-BrO_x$ interactions and nitrate production

In the conditions of the Arctic springtime, the basic chemistry of ozone and nitrogen oxides, presented above, is profoundly modified. Here we briefly review some elements of the $HO_x-NO_x-BrO_x$ interactions with a focus on the atmospheric conditions relevant to our sampling campaign.

4.3.1 Sources of HO_x and NO_x

To the best of our knowledge, the HO_x speciation (i.e. the OH/HO_2 partitioning) in the Arctic troposphere in springtime has never been measured directly. Therefore the HO_x budget relies only on modeling calculations, which do not always include up-to-date chemical mechanisms and processes. It appears that the five dominant sources of HO_x are the photolysis of HCHO, ozone, HOBr and HONO, and the reaction between HCHO and Br (Evans et al., 2003; Lehrer et al., 2004). HCHO and HONO are emitted by the seasonal

snowpack (Sumner and Shepson, 1999; Zhou et al., 2001). The relative magnitude of these pathways depend on actinic fluxes and levels of reactants for the photolytic sources, and on the intensity of the bromine chemistry for the last one. Overall, there is a large degree of interconversion between the HO_x family and BrO_x, mainly through HOBr. This species acts as a short-lived reservoir species for both families (Evans et al., 2003).

NO_x sources in the Arctic include global NO_x sources (long range transport (in the form of PAN) from the industrialized mid-latitude countries, lightning, soil emissions) but also a significant local component, namely snowpack emissions (Beine et al., 2002). These emissions, driven by sunlight and temperature-dependent equilibria, sustain the photochemical cycles involving NO_x when the NO_x pool originating from "classical" sources is exhausted for various reasons, including rapid oxidation into inorganic nitrate due to Arctic specific processes (Evans et al., 2003, see below).

4.3.2 Oxidation of NO by BrO

The reaction $BrO + NO \rightarrow NO_2 + Br$ competes with reactions (R3) and (R4), in terms of NO oxidation. Indeed, when comparing the oxidation rates of NO by BrO and O_3 (Atkinson et al., June 2006 version) for the conditions of the Arctic boundary layer (temperatures ranging between 236 and 269 K), one finds that 1 pmol mol^{-1} BrO has the same oxidizing power as 2–4 nmol mol^{-1} O_3 in oxidizing NO. This is of particular significance during ODEs, when the ozone mixing ratio drops to a few nmol mol^{-1} and BrO levels can sometimes reach over 10 pmol mol^{-1}.

4.3.3 Additional nitrate formation pathways

In addition to the general overview given in Sect. 4.1 with regards to the formation of nitrate, two more processes are to be considered in the Arctic troposphere in springtime :

1. HNO_4 heterogeneous chemistry

   HNO_4 is a NO_x reservoir species formed by reaction of NO_2 with HO_2, which is thermally relatively stable in the temperature range expected in the Arctic troposphere in springtime. In the aqueous phase, it reacts with a variety of compounds (HSO_3^-, HNO_2, Cl^-, Br^- and I^-) to form nitrate (Evans et al., 2003, and references therein). In Arctic conditions outside of the ODEs period, Evans et al. (2003) modeled this pathway to account for up to 40% of the NO_x sink, hence the nitrate production.

2. $BrONO_2$ hydrolysis

   When halogen radicals are present in the Arctic troposphere, an increasing body of evidence points towards the $BrONO_2$ hydrolysis as a major source of nitrate, through the heterogeneous reaction (Hanson et al., 1996; Sander et al., 1999) :

   $$BrONO_2 + H_2O \rightarrow HNO_3 + HOBr \quad \text{(R11)}$$

   The role of $BrONO_2$ has been mainly investigated for its important role in recycling Br during ODEs (Fan and Jacob, 1992). Its concomitant impact on nitrate formation has not attracted the same attention until recently. In a modeling effort mostly focused on gas-phase mechanisms, Calvert and Lindberg (2003) showed that $BrONO_2$ would be the most abundant N-containing species in the Arctic boundary layer. A more comprehensive study by Evans et al. (2003) shows that during ODEs the formation and hydrolysis of $BrONO_2$ could be responsible for the exhaustion of NO_x, that was observed by Beine et al. (1997).

5 Isotopic signatures of processes and species

To infer $\Delta^{17}O$ of nitrate from the atmospheric chemistry considerations presented above, it is necessary to know the isotopic composition of its precursors, and the rate of transfer of the isotope anomaly through the relevant oxidation pathways. In this approach, the most important variable is the isotopic composition of ozone because it is the overwhelmingly predominant source of isotope anomaly in the troposphere (Thiemens, 2006).

5.1 $\Delta^{17}O$ in bulk ozone

Unfortunately, no systematic measurement of $\Delta^{17}O(O_3)$ in the troposphere has ever been undertaken, despite the intense research effort devoted to the study of isotope anomalies in a wide range of species (e.g. nitrate, sulphate), all of which gain a substantial part of their isotope anomaly from reactions between their precursors and ozone. To the best of our knowledge, only two studies report triple isotopic measurements of ozone in the troposphere (Johnston and Thiemens, 1997; Krankowsky et al., 1995). Krankowsky et al. (1995) sampled air at an unidentified urban site (near Heidelberg, Germany, according to Brenninkmeijer et al. (2003)), and Johnston and Thiemens (1997) carried out three field studies in various environments: urban extremely polluted (Pasadena, California, USA), polluted marine boundary layer (La Jolla, California, USA) and remote desertic (White Sand Missile Range, New Mexico, USA). In order to compare the data published by Krankowsky et al. (1995) and Johnston and Thiemens (1997), we digitized the three-isotope plots from Krankowsky et al. (1995) (to obtain the individual $\delta^{18}O$ and $\delta^{17}O$ values) and calculated $\Delta^{17}O$ using the Eq. (1) for each sample. We find that the $\Delta^{17}O(O_3)$ data from Krankowsky et al. (1995) range from 6 to 54 ‰ (in average (25 ± 12) ‰). For the Johnston and Thiemens (1997) data we find $\Delta^{17}O(O_3) = (21 \pm 2)$ ‰ at Pasadena, $\Delta^{17}O(O_3) =$

(26±5) ‰ at La Jolla and $\Delta^{17}O(O_3)$= (32±4) ‰ at White Sand Missile Range. The main characteristics of all these data obtained in four different environments are reported in the Fig. 6. In all cases, there is a large scatter in $\Delta^{17}O(O_3)$ values, with very different average values at the different sampling sites.

Two interpretations of these differences are possible : either the $\Delta^{17}O(O_3)$ variability is "real" or it is purely a consequence of measurements artifacts. As we show below, it is currently virtually impossible to decipher the causes for the variability in the measured $\Delta^{17}O(O_3)$ values.

Firstly, the considerable scatter in the data produced so far (Krankowsky et al., 1995; Johnston and Thiemens, 1997) might originate from random errors and hence may not be representative of real variations in $\Delta^{17}O(O_3)$, as pointed out by Brenninkmeijer et al. (2003). This approach is substantiated by the averaging method used by these authors : indeed, when merging the three datasets of Johnston and Thiemens (1997), one finds that $\Delta^{17}O(O_3)$ = (27±5) ‰, a value comparable to what was calculated from Krankowsky et al. (1995). Contrary to Brenninkmeijer et al. (2003) we report here standard deviations and not errors of the mean since nothing unambiguously proves that random errors are the only cause for the variability in the measured $\Delta^{17}O(O_3)$.

The only variable widely accepted to influence the $\Delta^{17}O(O_3)$ value in the ozone formation process is the temperature of formation of ozone. A linear regression of the $\Delta^{17}O(O_3)$ values published by Morton et al. (1990) (augmented with one data point from Tuzson (2005)) against the temperature at which ozone was formed during their laboratory experiments yields : $\Delta^{17}O(O_3)$/‰= (0.08±0.02) T/K + (15±5) (R^2 = 0.8, n=6). Therefore $\Delta^{17}O$ variations of 10 ‰ would require temperature changes on the order of over 100 K. It is therefore unlikely that temperature differences are the driving factor behind the differences in $\Delta^{17}O$ among the different sampling sites. Furthermore, Krankowsky et al. (1995) explicitly stated that the variations in $\Delta^{17}O(O_3)$ were not correlated with temperature changes.

However, in light of the measurements of Johnston and Thiemens (1997), it could be argued that another process accounting for the variability in $\Delta^{17}O(O_3)$ has been left out. Indeed, while average values differ markedly from one site to another (see above), it should also be noted that, when plotted in a three-isotope plot, the data from the three sites shown by Johnston and Thiemens (1997) do align on lines featuring different slopes. Johnston and Thiemens (1997) proposed this as a proof that different ozone decomposition pathways induced different triple isotope effects. On the contrary, Brenninkmeijer et al. (2003) consider this as an additionnal reason to question the robustness of the data presented by Johnston and Thiemens (1997). Hence there is no consensus on the tropospheric value of $\Delta^{17}O(O_3)$ and the causes for its variations.

Even if the existence of the isotope anomaly in tropospheric ozone is not questioned here, it is particularly useful to recognize that, to date, its quantification carries a significant part of uncertainty. As a consequence, to interpret quantitatively $\Delta^{17}O$ measurements of atmospheric species, strong assumptions have to be made regarding the value of $\Delta^{17}O(O_3)$ and its variability. For instance, in all their publications, Michalski and coworkers (see e.g. Michalski et al., 2003, 2005 and references therein) chose a constant value of $\Delta^{17}O(O_3)$= 35 ‰, on behalf of *ad hoc* modeling calculations performed by Lyons (2001), but recently questioned by Zahn et al. (2006). Such an approach significantly hampers the strength of the conclusions reached in these studies. However, using a constant value for $\Delta^{17}O(O_3)$ at a given site throughout the year allowed for a detailed analysis of the seasonal trends in $\Delta^{17}O$ of atmospheric nitrate, that were successfully attributed to changes in its formation pathways (Michalski et al., 2003).

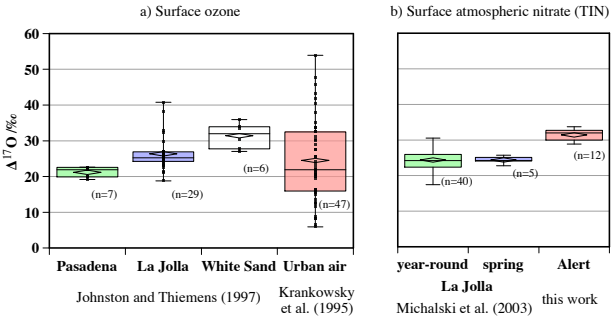

Fig. 6. (a) Overview of existing measurements of $\Delta^{17}O(O_3)$ in the troposphere. The box plot indicates the median, interquartile range, maximum and minimum values (every dot corresponds to a single measurement). The mean value is displayed (diamond symbol), as well as the number of data-points corresponding to each sampling site. **(b)** Isotope anomalies measured in nitrate during two measurement campaigns (Michalski et al., 2003, this study) are displayed as a comparison both in terms of average values and standard deviation within each sampling site.

In what follows, we assume a constant $\Delta^{17}O(O_3)$ value throughout our sampling campaign. Neverthless, to reduce the weakness of a reasoning based upon a single value for $\Delta^{17}O(O_3)$, which might not be representative of the isotopic composition of ozone in the Arctic troposphere, we use a range of $\Delta^{17}O(O_3)$ values, spanning between 25 and 35 ‰.

5.2 The intra-molecular distribution of $\Delta^{17}O$ in ozone

It is known that the intramolecular distribution of heavy oxygen atoms in the molecule of ozone differs from a stochastically expected distribution (Janssen, 2005). The asymmetric isotopologues of ozone are enriched in heavy oxygen isotopes with respect to bulk ozone, thus the terminal atoms of the molecule carry a higher load of heavy isotopes. Lyons (2001) was the first to compute the implications of this observation in terms of $\Delta^{17}O$, extrapolating to $^{49}O_3$ the different kinetic rates observed for ozone

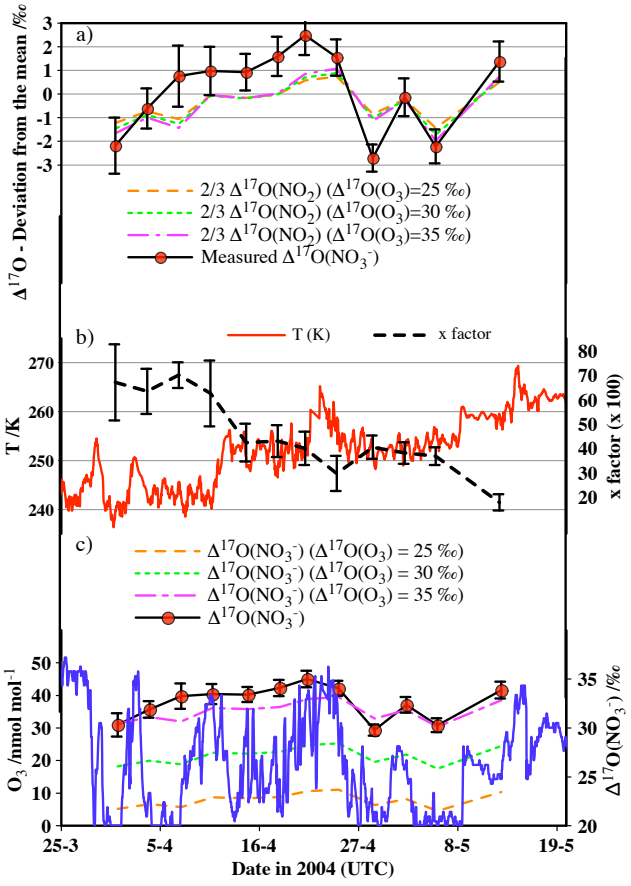

Fig. 7. **(a)** Comparison of the deviation from the mean of 2/3 $\Delta^{17}O(NO_2)$ with deviations from the mean of $\Delta^{17}O(NO_3^-)$. This shows that most of the variability of $\Delta^{17}O(NO_3^-)$ is captured by our estimate of the $\Delta^{17}O(NO_2)$ values over the measurement campaign. **(b)** Evolution of temperature and the x factor (which represents the degree of equilibration of OH with tropospheric water vapor in terms of $\Delta^{17}O$. c) Comparison of the calculated value of $\Delta^{17}O(NO_3^-)$ with the measured value, in the case where 100% of nitrate comes from the $BrONO_2$ hydrolysis, for the three $\Delta^{17}O(O_3)$ values considered in this study.

isotopologues formation (namely $^{50}O_3$ and $^{48}O_3$) published by Janssen et al. (1999). In the lower troposphere, taking $\Delta^{17}O(O_3)$= 35 ‰, he proposed that the asymmetric ozone molecule could bear an anomaly on the order of 85 ‰. Recently, using updated kinetic rates and a more balanced approach, Zahn et al. (2006) proposed that the terminal atom in the ozone molecule should feature an anomaly on the order of 39 ‰ (for a mean isotope anomaly of 34 ‰, i.e. $\Delta^{17}O(O_3, \text{terminal})=1.2\times\Delta^{17}O(O_3, \text{bulk})$). For this study we take :

– $\Delta^{17}O(O_3, \text{bulk})$= 25, 30 and 35 ‰

– $\Delta^{17}O(O_3, \text{terminal})$=30, 36 and 42 ‰, respectively.

5.3 $\Delta^{17}O(BrO)$

BrO is exclusively formed by reaction of bromine with ozone, thus it solely gains its isotope anomaly from this reaction. Theoretical considerations based on kinetic measurements (Toohey et al., 1988) and molecular crossed beam studies (Zhang et al., 1997) show that the reaction $Br + O_3 \rightarrow BrO + O_2$ is direct, and that the Br atom most likely attacks a terminal ozone atom. Therefore, it is expected that, at steady state during ODEs, the isotope anomaly of BrO is the same as the anomaly of the terminal atom in ozone, i.e. $\Delta^{17}O(BrO)$= 30, 36 and 42 ‰ for $\Delta^{17}O(O_3)$ = 25, 30 and 35 ‰, respectively. An experimental confirmation of this prediction is strongly needed, but it seems that BrO could carry the highest isotope anomaly in a chemically active molecule (other than ozone) in the troposphere. Given the increasing influence given to BrO in chemical mechanisms implemented in atmospheric models (e.g. Platt and Hönninger, 2003; von Glasow et al., 2004; Lary, 2005), this potentially unique isotopic signature could represent a tool of choice to test these hypotheses.

5.4 $\Delta^{17}O(RO_2)$

R represents H or any organic radical, so RO_2 represents the whole $HO_x - RO_x$ radical family - with the notable expection of OH, in terms of kinetics and isotopic composition. In processes known to occur at mid-latitudes, peroxy radicals are derived from atmospheric O_2 (e.g. Finlayson-Pitts and Pitts, 2000), so that Michalski et al. (2003) identified $\Delta^{17}O(RO_2)$ with that of atmospheric O_2 (-0.3 ‰, Barkan and Luz, 2005). Given the large uncertainties stated above in terms of the ozone isotope composition and the observed range in the isotope anomaly in nitrate (> 20 ‰), such a low deviation from the terrestrial fractionation line is insignificant, and therefore a value of $\Delta^{17}O(RO_2)$ = 0 ‰ was chosen.

Due to the high level of chemical interchange between the members of the HO_x family (namely OH and HO_2), it could be expected that their photochemical equilibrium results in a similar isotope anomaly. However, from the analysis of the chemical mechanisms leading to the formation of HO_2 from OH we observe that for the main reaction channel (i.e. $CO+OH \rightarrow H+CO_2$, followed by $H+O_2 \rightarrow HO_2$) the oxygen atoms incorporated in HO_2 derive from ambient molecular oxygen. To the best of our knowledge, in the Arctic troposphere only two processes could produce anomalous HO_2, namely the reaction of OH with BrO and O_3. However, the reaction of OH with CO dominates over each of them regardless the mixing ratios of the species in concern within their typical range : BrO (2–5 pmol mol^{-1}, Hönninger and Platt, 2002), O_3 (1–50 nmol mol^{-1}) and CO (150–160 nmol mol^{-1}, Evans et al., 2003, D. Worthy, personal communication, 2006). Therefore both channels leading to nonzero $\Delta^{17}O(HO_2)$ are negligible, as confirmed by the detailed analysis by Cantrell et al. (2003). Therefore

there is a strong isotopic decoupling within the HO_x family. The final step of other channels leading to HO_2 (HCHO photolysis (Lehrer et al., 2004), reaction of HCHO with Br (Evans et al., 2003)) is always the reaction between H and ambient molecular oxygen. From all of these processes, even if there is no consensus on their relative magnitude by lack of specific measurements and detailed analysis, with a good level of confidence it can be assumed that $\Delta^{17}O(HO_2)$= 0 ‰.

The same conclusion applies also for other members of the peroxy family (RO_x). Indeed, they are formed by reaction of a radical R with O_2 and therefore bear no significant isotope anomaly. The only modification induced by the presence of halogen atoms in the atmosphere occurs in the first step of the oxidation mechanism, during which not only OH but also halogen atoms abstract one hydrogen atom from hydrocarbon compounds (RH+X yields R+HX, where X represents Cl or Br). This has no implication on the isotopic composition of alkyl-peroxy, but significantly affects their chemical budget (Evans et al., 2003). From this point on, we assume $\Delta^{17}O(RO_2)$= 0 ‰.

There is evidence that $\Delta^{17}O(HO_2)$ is not strictly equal to zero, since rainwater H_2O_2 -an important end-product of peroxy radicals - was measured to carry an isotope anomaly on the order of 0–2 ‰ (Savarino and Thiemens, 1999a). However, such a value is not discernibly different from zero in the framework of our analysis.

5.5 $\Delta^{17}O(OH)$

Based on the above reasoning we assume that $\Delta^{17}O(RO_2)$ is approximately equal to 0 ‰. The case of OH is quite different, since several processes significantly contributing to the formation of OH are likely to transfer a non-zero isotope anomaly.

In the Arctic troposphere in springtime, net OH production proceeds through the reaction of $O(^1D)$ and H_2O (following ozone photolysis), the reaction between HO_2 and NO or O_3, and the direct photolysis of HONO and HOBr. Sheppard and Walker (1983) have shown that $O(^1D)$ produced by the photolysis of ozone was mostly (> 90 %) derived from a terminal oxygen atom. Under the assumption that the photolysis of ozone does not induce mass-independent fractionation, it is therefore expected that in OH produced through the reaction $O(^1D) + H_2O \rightarrow 2OH$, $\Delta^{17}O(OH) \simeq 0.5 \times \Delta^{17}O(O(^1D))$. This yields $\Delta^{17}O(OH) \simeq 15$, 18 and 21 ‰ for $\Delta^{17}O(O_3)$ = 25, 30 and 35 ‰, respectively. The reactions between ozone and HO_2, and NO and HO_2, do not result in a transfer of oxygen atom from ozone and NO to the produced OH, but rather an abstraction of one oxygen atom of HO_2 to form two O_2 molecules and NO_2, respectively. Therefore in these cases $\Delta^{17}O(OH) = \Delta^{17}O(HO_2) = 0$ ‰. Evaluating the isotopic composition of HOBr is complicated by the fact that several reactions lead to its production. On one hand, from the reaction between BrO and HO_2, one expects $\Delta^{17}O(HOBr) = \Delta^{17}O(BrO)$. On the other hand, HOBr produced heterogeneously during the hydrolysis of $BrONO_2$ drawns its oxygen atom from the surrounding water, with no isotope anomaly (see Sect. 7.2.4). The balance between theses mechanisms controls $\Delta^{17}O(HOBr)$ and, hence, $\Delta^{17}O(OH)$ formed by its photolysis. The same complex picture applies for the photolysis of HONO, since the mechanism responsible for their release from the snowpack is far from being understood (Zhou et al., 2001; Beine et al., 2006). The main precursor of HONO produced in the snowpack is atmospheric inorganic nitrate, whose isotope anomaly is known. However the fate of nitrate oxygen isotopes during its photolysis in the snowpack, and the subsequent release as NO_x or HONO is currently unknown and should depend on the chemical composition of the snow (McCabe et al., 2005; Savarino et al., 2006). Therefore we cannot estimate the $\Delta^{17}O$ value of the produced OH.

Dubey et al. (1997) studied the kinetics of the isotopic exchange reaction between OH and H_2O (in the case of the scrambling reaction $^{18}OH + H_2^{16}O \rightarrow H_2^{18}O + ^{16}OH$). We assume that the same rate of isotope exchange applies for ^{17}O, hence, for $\Delta^{17}O$ (Michalski et al., 2003). Given the fact that H_2O represents an enormous non-anomalous oxygen reservoir in the atmosphere with respect to OH, such a reaction tends to erase the isotope anomaly of OH. Regardless of the isotopic signature of the processes leading to the net production of OH radicals (which does not include the gross production from the interconversion between OH isotopologues via isotope equilibration with H_2O), the degree of equilibration of the isotope anomaly of the produced OH can be determined by the competition between the isotopic equilibration reaction and the OH net sink reactions. In their study on atmospheric nitrate formation in California, Michalski et al. (2003) showed that the equilibration process was always faster than all OH net sinks, and therefore considered $\Delta^{17}O(OH)$ = 0 ‰. We denote $\Delta^{17}O(OH)_{prod.OH}$ the isotope anomaly of the produced OH, and $\Delta^{17}O(OH)$ the isotope anomaly of OH at steady state. We denote $L^\dagger$ the net chemical loss rate (net chemical loss term divided by the OH concentration) :

$$L^\dagger = k_{OH+CO} \times [CO] + k_{OH+CH_4} \times [CH_4]$$

We denote x the fraction of the net loss with respect to the total loss (net + gross, that is the sum of isotopic exchange reaction term and the net chemical loss term) :

$$x = \frac{L^\dagger}{L^\dagger + k_{OH+H_2O} \times [H_2O]}$$

Assuming that all chemical sinks do not intrinsically induce mass-independent fractionation for OH, the isotope anomaly of OH at steady state is :

$$\Delta^{17}O(OH) = x \times \Delta^{17}O(OH)_{prod.OH} \quad (2)$$

Stated simply, if the isotopic exchange reaction dominates over net chemical losses (i.e. $x \ll 1$), then $\Delta^{17}O(OH)$

= 0 ‰. On the contrary, if net chemical losses dominate over the isotopic equilibrium reaction, then $\Delta^{17}O(OH) = \Delta^{17}O(OH)_{prod.OH}$. To assess the degree of suppression of the isotope anomaly acquired during the formation of OH, we compute the value of the x factor during our measurements campaign, using temperature, humidity, the mixing ratio of CO and CH_4 measured at Alert (D. Worthy, personal communication, 2006) and temperature dependent kinetic rates (Atkinson et al., June 2006 version; Dubey et al., 1997). The absolute water vapor concentration was deduced from relative humidity and temperature measurements using Bolton (1980) (i.e. $P_{water}=6.112e^{\frac{17.67\times(T-273)}{T-29.5}}$, with P_{water} in hPa and T in K). Similarly to the ozone mixing ratio measurements, the values for the x factor were averaged over each sampling period. The result of this calculation is shown on Fig. 7b). Contrary to lower latitude locations where this factor is always negligibly small and leads to $\Delta^{17}O(OH)$ = 0 ‰ year-round (Michalski et al., 2003), the x factor deviates significantly from zero during the measurement campaign. Polar regions are the only place where the troposphere is dry and cold enough to feature elevated values of the x factor. In this regard, the situation encountered here is similar to the OH isotopic budget of the stratosphere : indeed, the dryness and the low temperature prevailing in the stratosphere have led modelers to predict significant isotope anomalies in the stratosphere up to 40 ‰ according to Lyons (2001), above 30 ‰ for Zahn et al. (2006). Due to the increase of temperature and the concomitant increase of the water vapor content and to the high temperature dependency of the isotopic equilibrium (Dubey et al., 1997), the x factor exhibits a marked decrease over the course of the measurement campaign, from values around 70 % at the beginning of the measurement campaign to values lower than 20 % at the end of the campaign. Therefore, if OH was produced with a significant isotope anomaly, this anomaly would be present at the beginning of the measurement campaign but would have largely disappeared toward the end of the campaign.

6 Implications for $\Delta^{17}O(NO_2)$

We now examine the competition between the three major NO oxidants identified in the Arctic troposphere in springtime (O_3, RO_2 and BrO), in terms of kinetics and the subsequent influence on the isotopic composition of oxygen in NO_2.

The reactions between NO and BrO or RO_2 are isotopically easy to account on a mass-balance perspective. BrO transfers all of its isotope anomaly to NO_2 because it simply transfers all of its oxygen content. RO_2 does not transfer any isotope anomaly to NO_2 since $\Delta^{17}O(RO_2)$ = 0 ‰. The case of the reaction between O_3 and NO is more complex. The rate of transfer of isotope anomaly during this reaction depends simultaneously on mechanistic and isotopic considerations. Indeeed, the position of the oxygen atoms among the ozone molecule determines both their isotopic composition and their probability of reaction with NO. Since little is known regarding both the chemical mechanism for this reaction and the intramolecular isotope distribution in ozone, contradictory parameterizations have been published so far in various modeling studies. For some authors (see e.g. Lyons, 2001; Zahn et al., 2006), only the terminal atom of ozone reacts with NO to yield NO_2, although there is mechanistic evidence that the central atom of ozone also reacts with NO (see e.g. van den Ende et al., 1982, recently discussed by Savarino et al., 2006). Consistent with Savarino et al. (2006), in lack of a precise evaluation of the rate of transfer of the isotope anomaly of O_3 to NO_2, we vary this rate of transfer from 0.8 to 1.2, i.e. at photochemical equilibrium with only NO_x and ozone, $\Delta^{17}O(NO_2) = y \times \Delta^{17}O(O_3)$, with $y = 1\pm0.2$.

In the following part, we calculate steady-state abundance ratios for a given NO_2 isotopologue using the kinetic equations derived from the photochemical cycling of NO_x and ozone, disturbed by peroxy radicals and bromine oxides. We neglect species containing more than one heavy O atom (^{17}O or ^{18}O) because of their extremely low abundances. In addition, in the kinetic equations for NO and NO_2, NO_x sink terms such as the formation of HNO_3 are negligible compared to the $NO-NO_2$ interconversion terms. Indeed, the NO and NO_2 chemical lifetime (about a min) is much shorter than NO_x lifetime (about a day).

Q denotes ^{17}O or ^{18}O, and O represents ^{16}O. We additionally assume that kinetic rates (k values) and photolysis frequencies (J values) are the same for all O-isotopologues of a given species. For brevity, we denote $[RO_2]^\dagger=k_{NO+RO_2}[RO_2]$, $[ROQ]^\dagger=k_{NO+RO_2}[ROQ]$, $[BrO]^\dagger=k_{NO+BrO}[BrO]$, $[BrQ]^\dagger=k_{NO+BrO}[BrQ]$, $[O_3]^\dagger=k_{NO+O_3}[O_3]$ and $[O_2Q]^\dagger=k_{NO+O_3}[O_2Q]$, where [X] represents the sum of atmospheric concentrations of the isotopomers of a given species X.

$$\frac{d}{dt}[NO] = \frac{1}{2}J[NOQ] + J[NOO] - [NO] \times ([O_3]^\dagger + [BrO]^\dagger + [RO_2]^\dagger + y \times [O_2Q]^\dagger + [BrQ]^\dagger + [ROQ]^\dagger) \quad (3)$$

$$\frac{d}{dt}[NOO] = -J[NOO] + [NO] \times ([O_3]^\dagger + [RO_2]^\dagger + [BrO]^\dagger + \frac{3-y}{3}[O_2Q]^\dagger + \frac{1}{2}[ROQ]^\dagger) \quad (4)$$

Assuming steady-state and adding Eqs. (3) and (4) yields:

$$[NO]=\frac{1}{2}\frac{J[NOQ]}{\frac{y}{3}[O_2Q]^\dagger + \frac{1}{2}[ROQ]^\dagger + [BrQ]^\dagger}$$

Substituting [NO] in Eq. (4) yields, after rearranging:

$$\frac{1}{2}\frac{[NOQ]}{[NOO]}=\frac{\frac{y}{3}[O_2Q]^\dagger+\frac{1}{2}[ROQ]^\dagger+[BrQ]^\dagger}{[O_3]^\dagger+[RO_2]^\dagger+[BrO]^\dagger+\frac{3-y}{3}[O_2Q]^\dagger+\frac{1}{2}[ROQ]^\dagger}$$

In the equation above, $\frac{[O_2Q]^\dagger}{[O_3]^\dagger} \ll 1$ and $\frac{[ROQ]^\dagger}{[RO_2]^\dagger} \ll 1$, and $[O_3]^\dagger+[RO_2]^\dagger+[BrO]^\dagger = 1/\tau_{NO}$, where τ_{NO} is the chemical lifetime of NO. This equation can therefore be approximated and simplified into :

$$\frac{1}{2}\frac{[NOQ]}{[NOO]} = \tau_{NO} \times \left(\frac{y}{3}[O_2Q]^\dagger + \frac{1}{2}[ROQ]^\dagger + [BrQ]^\dagger\right) \quad (5)$$

The conversion of molecular fractions into atomic ratios is performed using the following equations :

$$\left(\frac{[Q]}{[O]}\right)_{O_3} = \frac{[O_2Q]}{3 \times [O_3]} \quad (6)$$

$$\left(\frac{[Q]}{[O]}\right)_{NO_2} = \frac{[NOQ]}{2 \times [NOO]} \quad (7)$$

$$\left(\frac{[Q]}{[O]}\right)_{BrO} = \frac{[BrQ]}{[BrO]} \quad (8)$$

$$\left(\frac{[Q]}{[O]}\right)_{RO_2} = \frac{[ROQ]}{2 \times [RO_2]} \quad (9)$$

Substituting (6), (7), (8) and (9) in Eq. (5), and applying the definition of $\Delta^{17}O$ (Eq. 1) gives, with $\Delta^{17}O(RO_2)$=0 ‰ :

$$\Delta^{17}O(NO_2) = \tau_{NO} \times \left(y[O_3]^\dagger \Delta^{17}O(O_3) + [BrO]^\dagger \Delta^{17}O(BrO)\right) \quad (10)$$

7 Nitrate formation pathways and $\Delta^{17}O(NO_3^-)$

The five pathways leading to nitrate from NO_2 (see Sect. 4) draw oxygen isotopes from different origins. The general mass balance equation governing the isotopic anomaly of nitrate can be expressed as:

$$\Delta^{17}O(NO_3^-) = 2/3 \times \Delta^{17}O(NO_2) + 1/3 \times \Delta^{17}O(O_{add.}) \quad (11)$$

where the first term on right-hand side of the equation represents the amount of isotopic anomaly originating from NO_2 and the second term, 1/3 $\Delta^{17}O(O_{add.})$, represents the isotope anomaly of the additional oxygen atom in nitrate that is acquired during the conversion of NO_2 into nitrate. This contribution obviously depends on the mechanism of conversion.

7.1 Isotope anomaly originating from NO_2

The estimation of $\Delta^{17}O(NO_2)$ values requires the knowledge of $[O_3]^\dagger$, $[BrO]^\dagger$ and $[RO_2]^\dagger$ and of their evolutions during the measurement campaign, through Eq. (10).

- $[O_3]^\dagger$ is easily derived from O_3 and temperature measurements carried out during the measurement campaign.
- $[BrO]^\dagger$: as explained in the Sect. 3.3, we take BrO = 2 pmol mol^{-1} as representative conditions for the BrO_x content of the lower atmosphere in the Arctic during ODEs.
- $[RO_2]^\dagger$: To the best of our knowledge no surface peroxy radical measurements have ever been undertaken at Alert in early spring and very little RO_x-HO_x data is available in the Arctic boundary layer during ODEs. Nonetheless, we calculate the evolution of RO_2 ratio during ODEs based on the field data acquired in the Arctic boundary layer during the campaign TOPSE 2000 (Tropospheric Ozone Production about the Spring Equinox experiment, see Atlas et al., 2003). Evans et al. (2003) summarized the boundary layer data acquired during TOPSE by binning mean measurements of species according to the ozone levels. According to Cantrell et al. (2003), the $[HO_2]/[RO_2]$ ratio was found to be more or less constant (0.75) during this whole campaign so that $[HO_2]$=0.75 $[RO_2]$. The dominant alkyl-peroxy radical is CH_3O_2 (Cantrell et al., 2003), so for the purpose of this study we take $[CH_3O_2]$=0.25 $[RO_2]$. In what follows, we therefore calculate k_{RO_2+NO}= 0.75k_{HO_2+NO} +0.25$k_{CH_3O_2+NO}$ so that RO_2 is treated as a virtual species integrating the combined kinetic rates of its two main components according to their relative abundances. Evans et al. (2003) showed that during ODEs, when the ozone mixing ratios drops from about 40 nmol mol^{-1} to 5 nmol mol^{-1} on average (consistent with our averaging approach), RO_2 concentrations decrease from (2.2±1.2) 10^8cm^{-3} to (1.3±0.6) 10^8cm^{-3}, corresponding roughly to a factor 2 division. At the same time, during ODEs, HCHO was found to drop by about a factor 4. This is consistent with the simplified RO_2 chemical budget described in Evans et al. (2003) where the main source of RO_2 is the photolysis of species such as HCHO, and the main sink is the self reaction RO_2+RO_2 (mainly HO_2+HO_2). Thus, at steady state, the RO_2 concentrations are expected to be proportional to the square root of the concentration of HCHO, which appears to be mostly the case during TOPSE 2000. HCHO mainly originates from the snowpack (Sumner and Shepson, 1999) and its drop during ODEs seems to be driven by reactions with halogen atoms, according to model studies (Evans et al., 2003). Overall, during ODEs, RO_2 concentrations drop by a factor much lower than the reduction factor of ozone concentrations (ca. factor 2 vs. factor 10). The data presented by Evans et al. (2003) are grouped in 4 ozone mixing ratios bins (<1 nmol mol^{-1}, 1 to 10 nmol mol^{-1}, 10 to 30 nmol mol^{-1}, and >30 nmol mol^{-1}). Since the average ozone mixing ratio did not drop below 5 nmol mol^{-1} during the sampling time, we do not consider here the bin corresponding to the lowermost ozone

mixing ratio. From these data, we observe that [RO_2] and [O_3] are positively correlated. To estimate the concentration of RO_2 as a function of the ozone mixing ratio at Alert during our measurement campaign, we apply the following relationship: $RO_2/10^8 cm^{-3}$=(0.09 O_3/nmol mol^{-1}+1.31)$^{1/2}$, and calculated the corresponding [RO_2]† accordingly, using temperature dependent kinetic rates from Atkinson et al. (June 2006 version).

From Eqs. (10) and (11) we can then estimate the value (averaged over all the samples) of the contribution of NO_2 to $\Delta^{17}O(NO_3^-)$: 2/3 $\Delta^{17}O(NO_2)$ = (12.6±0.7), (15.2±0.8) and (17.7±1.0) ‰ for $\Delta^{17}O(O_3)$ = 25, 30 and 35 ‰, respectively. Clearly, the isotopic anomaly on NO_2 can only account on average for about half of the measured $\Delta^{17}O(NO_3^-)$. Therefore, the rest of the isotopic anomaly should be acquired during the conversion of NO_2 into nitrate.

Although the isotope anomaly of NO_2 can only explain about half of the average measured $\Delta^{17}O(NO_3^-)$, it is still interesting to estimate its contribution to the temporal variability shown in Fig. 3. Fig. 7a) shows the temporal variations of the deviations from the mean for 2/3 $\Delta^{17}O(NO_2)$ and for measured $\Delta^{17}O(NO_3^-)$. For all the $\Delta^{17}O(O_3)$ values, we find a good correlation between 2/3 $\Delta^{17}O(NO_2)$ and the measured $\Delta^{17}O(NO_3^-)$ (R^2=0.7, n=12). The only deficiency is that the amplitude of variations in 2/3 $\Delta^{17}O(NO_2)$ is slightly smaller than that in measured $\Delta^{17}O(NO_3^-)$. It is worth pointing out that the variability in $\Delta^{17}O(NO_2)$ is found to be weakly dependent on the assumed value of $\Delta^{17}O(O_3)$ (see Fig. 7a). This indicates that the 20% uncertainty on the rate of transfer of the isotopic anomaly of O_3 to NO_2 (see Sect. 6) has relatively little impact on the variability of $\Delta^{17}O(NO_2)$. The overall results suggest that most of the variations in $\Delta^{17}O(NO_3^-)$ can be explained by the variations in $\Delta^{17}O(NO_2)$, which in turn are driven by the evolution of the ozone mixing ratio.

7.2 Isotope anomaly originating from the conversion of NO_2 into nitrate

This section is devoted to identifying the pathway of conversion of NO_2 into nitrate that can explain the part of the mean nitrate isotopic anomaly that cannot be accounted for by $\Delta^{17}O(NO_2)$ and that is represented by the term 1/3 $\Delta^{17}O(O_{add.})$ in Eq. (11).

Based on the estimations of mean $\Delta^{17}O(NO_2)$ presented above and using Eq. (11), it is possible to estimate the mean value of $\Delta^{17}O(O_{add.})$ required to account for the entire isotope anomaly of nitrate ($\Delta^{17}O(O_{add.})$ = 3 $\Delta^{17}O(NO_3^-)$ - 2 $\Delta^{17}O(NO_2)$). We find $\Delta^{17}O(O_{add.})$ = (56±3), (49±3) and (41±3) ‰ for $\Delta^{17}O(O_3)$ = 25, 30 and 35 ‰, respectively. This means that, within the framework of our simple model, regardless of the isotope anomaly of tropospheric ozone in this environment, $\Delta^{17}O(O_{add.})$ must exceed 40 ‰ to explain the measured $\Delta^{17}O(NO_3^-)$ values. Although 1/3 $\Delta^{17}O(O_{add.})$ represents the integrated contribution of all the pathways leading to nitrate, the pathways are first considered individually. We only focus on the contribution of the different conversion pathways to the nitrate isotope anomaly.

7.2.1 Mechanisms involving NO_3

NO_3 is a radical formed by reaction of NO_2 with O_3 (R6). It either abstracts a hydrogen atom from an hydrocarbon (R7), or reacts with NO_2 to form N_2O_5, which can undergo hydrolysis on any available water covered surface (R8). According to Peìro-Garcìa and Nebot-Gil (2003), the reaction between NO_2 and O_3 leads to the incorporation of a terminal oxygen atom from ozone to NO_3. Therefore, $\Delta^{17}O(NO_3)$ = 2/3 $\Delta^{17}O(NO_2)$ + 1/3 $\Delta^{17}O(O_3$, terminal).

Nitrate formed by abstraction of a hydrogen atom from a hydrocarbon should carry the same isotopic anomaly, giving $\Delta^{17}O(O_{add.})_{NO_3+RH}$= 30, 36 and 42 ‰ for $\Delta^{17}O(O_3)$ = 25, 30 and 35 ‰, respectively. These values are on the order of what is required to explain the measured $\Delta^{17}O(NO_3^-)$.

Nitrate produced through the heterogeneous hydrolysis of N_2O_5 carries a different isotope anomaly; a mass-balance equation shows that, taking into account the fact that $\Delta^{17}O(H_2O)$ = 0 ‰, $\Delta^{17}O(O_{add.})_{N_2O_5}$= 1/2 $\Delta^{17}O(O_3$, terminal) = 15, 18 and 21 ‰ for $\Delta^{17}O(O_3)$ = 25, 30 and 35 ‰, respectively. These values are too small to explain the entire magnitude of the measured $\Delta^{17}O(NO_3^-)$.

7.2.2 $OH + NO_2$

For the gas phase $OH + NO_2$ reaction, it is clear that, in the resulting nitrate, two oxygen atoms carry an isotopic signature corresponding to the parent NO_2, and one carries the isotopic signature of OH (Michalski et al., 2003), so that

$$\Delta^{17}O(O_{add.})_{OH+NO_2}=\Delta^{17}O(OH)$$

We have little information about the possible range of $\Delta^{17}O(OH)$ values in the Arctic atmosphere. We can consider the two extreme hypotheses (see Sect. 5.5). Either $\Delta^{17}O(OH)$ = 0 ‰ or small and, consequently, this pathway can be discounted. Or $\Delta^{17}O(OH)$ is very large, up to > 40 ‰, the critical value to explain the measured values of $\Delta^{17}O(NO_3^-)$. However, if the $OH + NO_2$ pathway was the major source of nitrate, $\Delta^{17}O(NO_3^-)$ should drop markedly over the course of the measurement campaign. Indeed, assuming at first order that the isotope anomaly of the OH source does not change, $\Delta^{17}O(OH)$ would be expected to drop by over a factor 3 during the campaign because of increasing temperatures and humidities (see Sect. 5.5). This would translate in a decrease of $\Delta^{17}O(NO_3^-)$ of more than 10 ‰ over the course of the measurement campaign if nitrate was produced through this pathway. The measurements do not show any temporal trend. Therefore, this pathway cannot account for our measured $\Delta^{17}O(NO_3^-)$.

7.2.3 HNO_4 hydrolysis

During the heterogeneous reaction of HNO_4 with a variety of compounds (see above, Sect. 4.3.3) to form nitrate, we assume that two atoms come from the initial NO_2, and one originates from the initial HO_2. Therefore,

$$\Delta^{17}O(O_{add.})_{HNO_4}=\Delta^{17}O(HO_2)$$

As $\Delta^{17}O(HO_2) \simeq 0$ ‰, this pathway cannot explain the measured $\Delta^{17}O(NO_3^-)$.

7.2.4 $BrONO_2$ hydrolysis

Experimental (Gane et al., 2001) and theoretical (McNamara and Hillier, 2001) studies of the $BrONO_2$ hydrolysis show that the O atom initially bounded to Br combines with the N atom in NO_2 to form nitrate, thus transferring the isotopic signature of BrO. In nitrate produced through this channel:

$$\Delta^{17}O(O_{add.})_{BrONO_2}=\Delta^{17}O(BrO)$$

Taking into account the fact that $\Delta^{17}O(BrO) = \Delta^{17}O(O_3, \text{terminal})$ (see Sect. 5.3), we find that $\Delta^{17}O(O_{add.})$ = 30, 36 and 42 ‰ for $\Delta^{17}O(O_3)$ = 25, 30 and 35 ‰, respectively. This range of values are on the order of what is required to explain the measured $\Delta^{17}O(NO_3^-)$.

7.3 Identification of the dominant pathways for nitrate formation

Only the NO_3+hydrocarbons pathway and the $BrONO_2$ hydrolysis pathway appear to be able to generate nitrate with isotope anomaly values compatible with the measurements. However, the fact that nitrate produced through these pathways carries an elevated isotopic anomaly is not sufficient. In order to attribute the magnitude of measured $\Delta^{17}O(NO_3^-)$ to these pathways, they also have to be the dominant pathways for nitrate formation. We therefore estimate and compare the chemical rates of the various pathways of nitrate formation in the context of ODEs in order to identify the dominant pathway.

Based on the fact that sunlight was permanent at the sampling site and in the Arctic basin during the whole campaign, we do not expect any significant levels of the night-time radical NO_3 to be present. Nonetheless, the analysis of the trajectories (Fig. 2) reveals that several air masses originate from locations further south where sunlight was not completely permanent. Some air masses could thus have experienced a bit of night-time conditions favorable to nitrate production via NO_3 channels at the beginning of their journey to the Alert. However, in this situation, the amount of nitrate produced would be minimal and, as this particulate nitrate would be produced at least several days before the air masses reach Alert, most of it would have been scavenged on the way and deposited south of Alert. Therefore, the pathways involving NO_3 are not considered to be a majour source of the nitrate sampled at Alert during our measurement campaign. This conclusion is supported by results from other studies. Michalski et al. [2003] found that the reaction between NO_3 and hydrocarbons (R7) did not account for more than 10% of the budget of nitrate in the context of a polluted marine boundary layer. In the Arctic, this proportion is expected to be much lower. Even if elevated NO_3 levels could be sustained in this environment, the competition with halogen atoms in terms of hydrocarbon oxidation would not be favorable to NO_3, thus limiting the rate of formation of nitrate though this pathway. Regarding the channel involving N_2O_5 hydrolysis, it seems clear from detailed model simulations supported by large-scale campaign measurements that this pathway is minor for the in-situ production of nitrate in the Arctic spring (Evans et al., 2003).

We are now left with three pathways for nitrate formation. The first step of each of these pathways can be summarized as follow:

$$XO + NO_2 \rightarrow XONO_2$$

with X denoting Br, OH and H.

$XONO_2$ then undergoes hydrolysis to form NO_3^-. Sink reactions for $XONO_2$ are photolysis (J_X) and heterogeneous deposition whose efficiency is determined by an heterogeneous removal rate (k_X) (Ridley and Orlando, 2003). At steady state, $[XONO_2]$ is given by :

$$[XONO_2]=\frac{k_{XO+NO_2}[XO][NO_2]}{J_X + k_X}$$

The production rate of inorganic nitrate (P_{XONO_2}) for each channel is equal to $k_X \times [XONO_2]$. We therefore have :

$$P_{XONO_2}=[NO_2]k_X\frac{k_{XO+NO_2}[XO]}{J_X + k_X} \quad (12)$$

Data found in the literature are used to estimate the relative importance of the different pathways. Temperature-dependent kinetic rates (k_{XO+NO_2}) are taken from Atkinson et al. (June 2006 version). Heterogeneous loss rates are taken from Ridley and Orlando (2003), i.e. $k_X = 2\,10^{-6}$, $1\,10^{-4}$ and 0.3 s^{-1} for X = H, OH and Br, respectively. Photolysis rates are calculated for the location of Alert on April 1 2004, at 12:00 UTC, using the TUV package (Madronich and Flocke, 1998). A OH concentration of $1\,10^6$ cm^{-3} is chosen in order to derive the upper limit of the chemical rate of the $OH + NO_2$ reaction (Sumner and Shepson, 1999). $[HO_2]$ is taken equal to $1.5\,10^8$ cm^{-3} (Evans et al., 2003; Cantrell et al., 2003), and a BrO mixing ratio of 2 pmol mol^{-1}, which is consistent with the rest of the study. Regardless of the temperature (in the range 240–270 K), we find that the $OH + NO_2$ pathway can account at best for up to 5% of the production of inorganic nitrate in this context. The hydrolysis of $BrONO_2$ and of HNO_4 are the two dominant sources of nitrate. This crude calculation does not allow us to identify the dominant pathway between these two

mechanisms because their rates of nitrate production are of the same order of magnitude. However, the fact that only the $BrONO_2$ hydrolysis among these two pathways can produce $\Delta^{17}O(NO_3^-)$ values, that are quantitatively consistent with the measurements (see Sect. 7.2), leads us to conclude that the hydrolysis of $BrONO_2$ is the major source of inorganic nitrate in the Arctic troposphere in springtime. This is in agreement with conclusions of recent modelling work by Evans et al. (2003) and Calvert and Lindberg (2003).

It is noteworthy, however, that even if 100% of the nitrate was to be produced through the $BrONO_2$ channel, a good match with the measured data would only be obtained for $\Delta^{17}O(O_3)$ on the order of 35‰. With the mechanism presented in this paper, we are unable to account for the observed elevated values of $\Delta^{17}O(NO_3^-)$ with a $\Delta^{17}O(O_3)$ value of ca. 25‰ as recommended by Brenninkmeijer et al. (2003). Indeed, even if all oxygen atoms incorporated in nitrate were to be drawn from terminal oxygen atoms of ozone, this would only give $\Delta^{17}O(NO_3^-)$ = 30‰ (assuming $\Delta^{17}O(O_3)$ = 25‰). This value is still 5‰ lower than some $\Delta^{17}O(NO_3^-)$ values measured at Alert. This stresses the need for new and accurate measurements of $\Delta^{17}O(O_3)$ throughout the troposphere, as well as a better characterization of the isotope anomaly transfer rates (e.g. during the reaction $NO + O_3 \rightarrow NO_2 + O_2$).

8 Conclusions

In spring 2004, total inorganic nitrate was collected at Alert, Nunavut, and its triple isotopic composition was measured. It appears that the isotope anomaly of nitrate records a footprint of the tropospheric ozone depletion events that occur during spring in this environment.

We extended to polar environments the framework first proposed by Michalski et al. (2003) for deciphering the origin of the variations in $\Delta^{17}O(NO_3^-)$ in the troposphere. We show that the correlation between $\Delta^{17}O(NO_3^-)$ and the ozone mixing ratio during ODEs is likely to originate from variations in $\Delta^{17}O(NO_2)$ brought about by changes in the relative importance of the three oxidation channels of NO, namely, oxidation by O_3, BrO and RO_2. We also show that our results are consistent with the fact that the hydrolysis of $BrONO_2$ is the major pathway for nitrate formation in this environment, on top of being a key species in the BrO recycling, during ODEs (Fan and Jacob, 1992). $\Delta^{17}O(NO_3^-)$ is more likely to vary because of changes in the kinetics and relative importance of oxidation pathways than changes in $\Delta^{17}O(O_3)$ itself. However, this should be tested critically in the field. The community desperately needs reliable measurements of $\Delta^{17}O(O_3)$ in a variety of atmospheric environments to corroborate, or not, this hypothesis, which constitutes the backbone (and the Achilles' heel) of such an approach. There is also the need for detailed chemistry-transport modelling. Some of the calculations presented here are only first-order estimations. Therefore, it appears possible that new results in the fast-moving research front on isotope anomalies in atmospheric species could modify substantially the conclusions reached here in light of information available at the present time.

Finally, our results can be interpreted in terms of the reaction of the atmospheric chemical system to a change in its oxidative power. One possible indicator of the oxidative power of the atmosphere is the chemical lifetime of NO. Indeed, its main oxidants are ozone, $HO_x - RO_x$ and halogen oxides, the three of them (along with H_2O_2) being the most prominent atmospheric oxidants. We showed in this study that $\Delta^{17}O(NO_3^-)$ was intricately coupled with the chemical lifetime of NO. For the conditions prevailing during this measurement campaign (BrO levels remaining rather low during ODEs, so no "bromine explosion"), the ozone mixing ratio drops were associated with a strong decrease in the oxidative power of the atmosphere. It has been suggested, in light of the first findings on the origin of the oxygen anomaly in nitrate, that the oxygen isotopic content of nitrate recorded in polar ice cores could be used as a proxy for past oxidative power, crucial to understanding of chemical feedbacks in the Earth climate system. The results of the present study make this idea appealing, even if the signature we recorded is associated with strong cases of ozone depletion. The sensitivity of $\Delta^{17}O(NO_3^-)$ to changes in the ozone mixing ratio is rather low (slope of (0.15 ± 0.03) ‰ / nmol mol^{-1}) and may not be suitable to study moderate changes in the ozone mixing ratio at the global scale. In addition, post-depositionnal effects within the firn and in the ice have to be studied very carefully in order to interpret $\Delta^{17}O(NO_3^-)$ records, and derive estimates of the past oxidant activity in the atmosphere (see the recent studies by Blunier et al., 2005 and McCabe et al., 2005).

Acknowledgements. We thank the staff at the GAW lab at Alert (and especially K. Anderson) who carried out the aerosol sampling. We gratefully thank J.-L. Jaffrezo, M. Baroni and J.-P. Balestrieri for analytical and technical assistance. The International Balzan Foundation and CRYOSTAT are acknowledged for their contribution to the IRMS purchase. The French Polar Institute (IPEV) and CEFIPRA/IFCPAR are acknowledged for their financial and scientific support. NILU and, in particular, A. Stohl are acknowledged for providing the FLEXTRA trajectories (http://www.nilu.no/trajectories) used in this study. S. Bekki thanks A. Bazureau for her help with the plotting of the trajectories. S. Morin thanks ÉNS and ENPC for financial support. We gratefully acknowledge J. Kaiser and one anonymous referee, whose insightful criticisms strongly improved the consistency of our manuscript. Comments by M. Piot and M. Frey were appreciated during the revision process of this manuscript.

Edited by: T. Röckmann

References

Alexander, B., Savarino, J., Kreutz, K. J., and Thiemens, M. H.: Impact of preindustrial biomass-burning emissions on the oxidation pathways of tropospheric sulfur and nitrogen, J. Geophys. Res., 109, D08303, doi:10.1029/2003JD004218, 2004.

Atkinson, R., Baulch, D. L., Cox, R. A., et al.: Summary of Evaluated Kinetic and Photochemical Data for Atmospheric Chemistry, available on line at http://www.iupac-kinetic.ch.cam.ac.uk/, June 2006 version.

Atlas, E., Ridley, B., and Cantrell, C.: The Tropospheric Ozone Production about the Spring Equinox (TOPSE) Experiment: Introduction, J. Geophys. Res., 108(D4), 8353, doi:10.1029/2002JD003172, 2003.

Baertschi, P.: Absolute ^{18}O Content of Standard Mean Ocean Water, Earth Planet. Sci. Lett., 31, 341, 1976.

Barkan, E. and Luz, B.: High-precision measurements of $^{17}O/^{16}O$ and $^{18}O/^{16}O$ ratios in H_2O, Rapid Commun. Mass Spectrom., 19, 3737–3742, 2005.

Barrie, L., Bottenheim, J., Rasmussen, R., Schnell, R., and Crutzen, P. J.: Ozone destruction and photochemical reactions at polar sunrise in the lower Arctic troposphere, Nature, 334, 138–141, 1988.

Beine, H. J., Jaffe, D. A., Stordal, F., Engardt, M., Solberg, S., Schmidbauer, N. and Holmen, K.: NO_x during ozone depletion events in the arctic troposphere at Ny Ålesund, Svalbard, Tellus Ser. B, 49, 556–565, 1997.

Beine, H. J., Honrath, R. E., Domine, F., Simpson, W. R., and Fuentes, J. D.: NO_x during background and ozone depletion periods at Alert: Fluxes above the snow surface, J. Geophys. Res., 107(D21), 4584, doi:10.1029/2002JD002082, 2002.

Beine, H. J., Amoroso, A., Domine, F., King, M. D., Nardino, M., Ianniello, A., and France, J. L.: Surprisingly small HONO emissions from snow surfaces at Browning Pass, Antarctica, Atmos. Chem. Phys., 6, 2569–2580, 2006.

Blunier, T., Floch, G., Jacobi, H., and Quansah, E.: Isotopic view on nitrate loss in Antarctic surface snow, Geophys. Res. Lett., 32, L13501, doi:10.1029/2005GL023011, 2005.

Böhlke, J., Mroczkowski, S., and Coplen, T.: Oxygen isotopes in nitrate: new reference materials for ^{18}O:^{17}O:^{16}O measurements and observations on nitrate-water equilibration, Rapid Commun. Mass Spectrom., 17, 1835–1846, 2003.

Bolton, D.: The computation of equivalent potential temperature, Monthly Weather Rev., 108, 1046–1053, 1980.

Bottenheim, J., Gallant, A., and Brice, K.: Measurements of NO_y species and O_3 at 82° N latitude, J. Geophys. Res., 13, 113–116, 1986.

Bottenheim, J., Fuentes, J., Tarasick, D., and Anlauf, K.: Ozone in the Arctic lower troposphere during winter and spring 2000 (ALERT2000), Atmos. Environ., 36, 2535–2544, 2002.

Bottenheim, J. W., Barrie, L. A., and Atlas, E.: The Partitioning of Nitrogen Oxides in the Lower Arctic Troposphere During Spring 1988, J. Atmos. Chem., 17, 15–27, 1993.

Bottenheim, J. and Chan, E.: A trajectory study into the origin of springtime Arctic boundary layer ozone depletion, J. Geophys. Res., 111(D19301), doi:10.1029/2006JD007055, 2006.

Brenninkmeijer, C. A. M., Janssen, C., Kaiser, J., Röckmann, T., Rhee, T. S., and Assonov, S. S.: Isotope Effects in the Chemistry of Atmospheric Trace Compounds, Chem. Rev. , 103 (12), 5125–5162, doi 10.1021/cr020644k S0009-2665(02)00644-1, 2003.

Calvert, G. and Lindberg, S.: A modeling study of the mechanism of the halogen/ozone/ mercury homogeneous reactions in the troposphere during the polar spring, Atmos. Environ., 37, 4467–4481, 2003.

Cantrell, C., Mauldin, L., Zondlo, M., et al.: Steady state free radical budgets and ozone photochemistry during TOPSE, J. Geophys. Res., 108, 8361, doi:10.1029/2002JD002198, 2003.

Domine, F. and Shepson, P.: Air-Snow Interactions and Atmospheric Chemistry, Science, 297, 1506–1510, 2002.

Dubey, M., Mohrschladt, R., Donahue, N., and Anderson, J.: Isotope Specific Kinetics of Hydroxyl Radical (OH) with Water (H_2O): Testing Models of Reactivity and Atmospheric Fractionation, J. Phys. Chem. A, 101, 1494–1500, 1997.

Evans, M. J., Jacob, D. J., Atlas, E., et al.: Coupled evolution of BrO_x-ClO_x-HO_x-NO_x chemistry during bromine-catalyzed ozone depletion events in the Arctic boundary layer, J. Geophys. Res., 108(D4), 8368, doi:10.1029/2002JD002732, 2003.

Fan, S.-M. and Jacob, D.: Surface ozone depletion in Arctic spring sustained by bromine reactions on aerosols, Nature, 359, 522–524, doi:10.1038/359522a0, 1992.

Finlayson-Pitts, B. J., and Pitts, J. N.: Chemistry of the Upper and Lower Atmosphere, Academic Press, 2000.

Gane, M., Williams, N., and Sodeau, J.: A Reflection-Absorption Infrared Spectroscopy (RAIRS) Investigation of the Low-Temperature Heterogeneous Hydrolysis of Bromine Nitrate, J. Phys. Chem A, 105, 4002–4009, 2001.

Hanson, D. R., Ravishankara, A. R., and Lovejoy, E. R.: Reaction of $BrONO_2$ with H_2O on submicron sulfuric acid aerosol and the implications for the lower stratosphere, J. Geophys. Res., 101D, 9063–9069, 1996.

Hastings, M., Steig, E. J., and Sigman, D. M.: Seasonal variations in N and O isotopes of nitrate in snow at Summit, Greenland: Implications for the study of nitrate in snow and ice cores, J. Geophys. Res., 109, D20306, doi:10.1029/2004JD004991, 2004.

Heaton, T., Wynn, P., and Tye, A.: Low $^{15}N/^{14}N$ ratios for nitrate in snow in the High Arctic (79° N), Atmos. Environ., 38, 5611–5621, 2004.

Holland, H. D.: The chemistry of the Atmosphere and the Oceans, Wiley, 1978.

Hönninger, G. and Bottenheim, J.: Reactive Halogen Studies by Long-term MAX-DOAS Observations at Alert, Nunavut, Eos. Trans. AGU, 84, A11F–0050, 2003.

Hönninger, G. and Platt, U.: Observation of BrO and its vertical distribution during surface ozone depletion at Alert, Atmos. Environ., 36, 2481–2489, 2002.

Hönninger, G., Morin, S., Staebler, R. M., and Bottenheim, J.: Reactive Bromine and Ozone Studies at Alert, Nunavut, Canada: Measurements at the Coast and Out On The Ice (OOTI2004), SOLAS Conference, Halifax, 2004.

Hopper, J., Barrie, L., Silis, A., Hart, W., Gallant, A., and Dryfhout, H.: Ozone and meteorology during the 1994 Polar Sunrise Experiment, J. Geophys. Res., 103, 1481–1492, 1998.

Jaffrezo, J., Calas, N., and Bouchet, M.: Carboxylic acids measurements with ionic chromatography, Atmos. Environ., 32, 2705–2708, 1998.

Janssen, C., Guenther, J., Krankowsky, D., and Mauersberger, K.: Relative formation rates of $^{50}O_3$ and $^{52}O_3$ in ^{16}O–^{18}O mixtures, J. Chem. Phys., 111, 7179–7182, 1999.

Janssen, C.: Intramolecular isotope distribution in heavy ozone

($^{16}O^{18}O^{16}O$ and $^{16}O^{16}O^{18}O$), J. Geophys. Res., 110, D08308, doi:10.1029/2004JD005479, 2005.

Johnston, J. and Thiemens, M. H.: The isotopic composition of tropospheric ozone in three environments, J. Geophys. Res., 102, 25 395–25 404, 1997.

Kaiser, J., Röckmann, T., and Brenninkmeijer, C.: Contribution of mass-dependent fractionation to the oxygen isotope anomaly of atmospheric nitrous oxide, J. Geophys. Res., 109, D03305, doi:10.1029/2003JD004088, 2004.

Krankowsky, D., Bartecki, F., Klees, G. G., Mauersberger, K., Schellenbach, K., and Stehr, J.: Measurement of heavy isotope enrichment in tropospheric ozone, Geophys. Res. Lett., 22, 1713–1716, 1995.

Lary, D.: Halogens and the chemistry of the free tropopshere, Atmos. Chem. Phys., 5, 227–237, 2005.

Lehrer, E., Wagenbach, D., and Platt, U.: Aerosol chemical composition during tropospheric ozone depletion at Ny Ålesund/Svalbard, Tellus B, 49B, 486–495, 1997.

Lehrer, E., Hönninger, G., and Platt, U.: A one dimensional model study of the mechanism of halogen liberation and vertical transport in the polar troposphere, Atm. Chem. Phys., 4, 2427–2440, 2004.

Li, W. J., Ni, B. L., Jin, D. Q., Zhang, Q. G.: Measurement of the Absolute Abundance of Oxygen-17 in V-SMOW, Kexue Tongbao, Chinese Science Bulletin, 33 (19), 1610, 1988.

Lyons, J.: Transfer of Mass-Independent Fractionation in Ozone to other Oxygen-containing Radicals in the Atmosphere, Geophys. Res. Lett., 28, 3231–3234, 2001.

Madronich, S., and Flocke, S.: The role of solar radiation in atmospheric chemistry, in: Handbook of Environmental Chemistry, edited by: P. Boule, Springer Verlag, Heidelberg, pp. 1-26, 1998.

Mauersberger, K., Lämmerzahl, P., and Krankowsky, D.: Stratospheric ozone isotope enrichments – revisited, Geophys. Res. Lett., 28, 3155–3158, 2001.

McCabe, J., Boxe, C., Colussi, A., Hoffman, M., and Thiemens, M.: Oxygen isotopic fractionation in the photochemistry of nitrate in water and ice, J. Geophys. Res., 110, D15310, doi:10.1029/2004JD005484, 2005.

McNamara, J. and Hillier, I.: Mechanism of the Hydrolysis of Halogen Nitrates in Small Water Clusters Studied by Electronic Structure Methods, J. Phys. Chem A, 105, 7011–7024, 2001.

Michalowski, B. A., Francisco, J. S., Li, S. M., Barrie, L. A., Bottenheim, J. W., and Shepson, P. B.: A computer model study of multiphase chemistry in the Arctic boundary layer during polar sunrise, J. Geophys. Res., 105, 15 131–15 146, 2000.

Michalski, G., Savarino, J., Bohlke, J. K., and Thiemens, M.: Determination of the total oxygen isotopic composition of nitrate and the calibration of a Delta O-17 nitrate reference material, Anal. Chem., 74, 4989–4993, 2002.

Michalski, G., Scott, Z., Kabiling, M., and Thiemens, M.: First measurements and modeling of $\Delta^{17}O$ in atmospheric nitrate, Geophys. Res. Lett., 30(16), 1870, doi:10.1029/2003GL017015, 2003.

Michalski, G., Bockheim, J., Kendall, C., and Thiemens, M.: Isotopic composition of Antarctic Dry Valley nitrate: Implications for NO_y sources and cycling in Antarctica, Geophys. Res. Lett., 32, L13817, doi:10.1029/2004GL022,121, 2005.

Miller, M.: Isotopic fractionation and the quantification of ^{17}O anomalies in the oxygen three-isotope system: an appraisal and geochemical significance, Geochim. Cosmochim. Acta, 66, 1881–1889, 2002.

Morin, S., Hönninger, G., Staebler, R. M., and Bottenheim, J. W.: A high time resolution study of boundary layer ozone chemistry and dynamics over the Arctic Ocean near Alert, Nunavut, Geophys. Res. Lett., 32, L08809, doi:10.1029/2004GL022098, 2005.

Morton, J., Barnes, J., Schueler, B., and Mauersberger, K.: Laboratory Sudies of Heavy Ozone, J. Geophys. Res., 95, 901–907, 1990.

Peìro-Garcìa, J. and Nebot-Gil, I.: *Ab Initio* Study of the Mechanism of the Atmospheric Reaction: NO_2+O_3 $\rightarrow$ NO_3 + O_2, J. Comput. Chem., 24, 1657–1663, 2003.

Platt, U. and Janssen, C.: Observation and role of the free radicals NO_3, ClO, BrO and IO in the troposphere, Faraday Discuss., 100, 175–198, 1995.

Platt, U. and Hönninger, G.: The role of halogen species in the troposphere, Chemosphere, 52, 325–338, 2003.

Ridley, B. A. and Orlando, J. J.: Active nitrogen in Surface Ozone Depletion Events at Alert during Spring 1998, J. Atmos. Chem., 44, 1–22, 2003.

Ridley, B., Walega, J., Montzka, D., et al.: Is the Arctic Surface Layer a Source and Sink of NO_x in Winter/Spring, J. Atmos. Chem., 36, 1–22, 2000.

Röckmann, T., Kaiser, J., Crowley, J. N., Brenninkmeijer, C. A. M., and Crutzen, P. J.: The origin of the anomalous or "mass-independent" oxygen isotope fractionation in tropospheric N_2O, Geophys. Res. Lett., 28, 503–506, 2001.

Sander, R., Vogt, R., Harris, G., and Crutzen, P.: Modeling the chemistry of ozone, halogen compounds, and hydrocarbons in the Arctic troposphere during spring, Tellus B, 49B, 522–532, 1997.

Sander, R., Rudich, Y., von Glasow, R., and Crutzen, P. J.: The role of $BrNO_3$ in marine tropospheric chemistry: A model study, Geophys. Res. Lett., 26, 2857–2860, 1999.

Sander, R., Burrows, J., and Kaleschke, L.: Carbonate precipitation in brine – a potential trigger for tropospheric ozone depletion events , Atm. Chem. Phys., 6, 4653–4658, 2006

Savarino, J. and Thiemens, M.: Analytical procedure to determine both $\delta^{18}O$ and $\delta^{17}O$ of H_2O_2 in natural water and first measurements, Atmos. Environ., 33, 3683–3690, 1999.

Savarino, J. and Thiemens, M.: Mass-Independent Oxygen Isotope (^{16}O, ^{17}O, ^{18}O) Fractionation Found in H_x, O_x Reactions, J. Phys. Chem. A, 103, 9221–9229, 1999.

Savarino, J., Kaiser, J., Morin, S., Sigman, D. M., and Thiemens, M. H.: Nitrogen and oxygen isotopic constraints on the origin of atmospheric nitrate in coastal Antarctica, Atmos. Chem. Phys. Discuss., 6, 8817–8870, 2006, http://www.atmos-chem-phys-discuss.net/6/8817/2006/.

Schaap, M., Müller, K., and ten Brink, H. M.: Constructing the European aerosol nitrate concentration field from quality analysed data, Atmos. Environ., 36, 1323–1335, 2002.

Sirois, A. and Barrie, L.: Arctic lower tropospheric aerosol trends and composition at Alert, Canada: 1980–1995, J. Geophys. Res., 104, 11 599–11 618, 1999.

Sheppard, M.G. and Walker, R.B.: Wigner method studies of ozone photodissociation, J. Chem. Phys., 78(12),7191–7199,1983.

Stohl, A.: Computation, accuracy and applications of trajectories – a review and bibliography, Atmos. Environ., 32, 947–966, 1998.

Stohl, A. and Seibert, P.: Accuracy of trajectories as determined

from the conservation of meteorological tracers., Quart. J. Roy. Meteorol. Soc., 124, 1465–1484, 1998.

Stohl, A., Wotawa, G., Seibert, P., and Kromp-Kolb, H.: Interpolation errors in wind fields as a function of spatial and temporal resolution and their impact on different types of kinematic trajectories, J. Appl. Meteorol., 34, 2149–2165, 1995.

Sumner, A. and Shepson, P.: Snowpack production of formaldehyde and its effect on the Arctic troposphere, Nature, 398, 230–233, 1999.

Tang, T. and McConnell, J.: Autocatalytic release of bromine from Arctic snow pack during polar sunrise, Geophys. Res. Lett., 23, 2633–2636, 1996.

Tarasick, D. and Bottenheim, J.: Surface ozone depletion episodes in the Arctic and Antarctic from historical ozonesonde records, Atmos. Chem. Phys., 2, 197–205, 2002, http://www.atmos-chem-phys.net/2/197/2002/.

Thiemens, M. H.: History and Applications of Mass-Independent Isotope Effects, Annu. Rev. Earth Planet. Sci. , 34, 217–262, 2006.

Thiemens, M. H. and Heidenreich III, J. E.: The Mass-Independent Fractionation of Oxygen: A Novel Isotope Effect and Its Possible Cosmochemical Implications, Science, 219, 1073–1075, 1983.

Toohey, D., Brune, W. H., and Anderson, J. G.: Rate constant for the Reaction $Br+O_3 \rightarrow BrO+O_2$ from 248 to 418 K: Kinetics and Mechanism, Int. J. of Chem. Kinet., 20, 131–144, 1988.

Tuzson, B.: Symmetry specific study of ozone isotopomer formation, PhD-Thesis, Ruprecht-Karls Universität, Heidelberg, 2005.

van den Ende, D., Stolte, S., Cross, J. B., Kwei, G. H., and Valentini, J. J.: Evidence for 2 Different Transition-States in the Reaction of $NO+O_3 \rightarrow NO_2^*+O_2$, J. Chem. Phys., 77, 2206–2208, 1982.

von Glasow, R., von Kuhlmann, R., Lawrence, M., Platt, U., and Crutzen, P. J.: Impact of reactive bromine chemistry in the troposphere, Atmos. Chem. Phys., 4, 2481–2497, 2004, http://www.atmos-chem-phys.net/4/2481/2004/.

Watts, S., Yaaqub, R., Davies, T., Lowenthal, D. H., Rahn, K. A., Harrison, R. M., Storr, B. T., and Baker, J. L.: The use of Whatman 41 filter papers for high volume aerosol sampling, Atmos. Environ., 21, 2731–2736, 1987.

Zahn, A., Franz, P., Bechtel, C., Grooß, J.-U., and Röckmann, T.: Modelling the budget of middle atmospheric water vapour isotopes, Atmos. Chem. Phys., 6, 2073–2090, 2006, http://www.atmos-chem-phys.net/6/2073/2006/.

Zeng, T., Wang, Y., Chance, K., Blake, N., Blake, D., and Ridley, B.: Halogen-driven low-altitude O_3 and hydrocarbon losses in spring at northern high latitudes, J. Geophys. Res., 111, D17313, doi:10.1029/2005JD006706, 2006.

Zhang, J., Miau, T.-T., and Lee, Y. T.: Crossed Molecular Beam Study of the Reaction $Br+O_3$, J. Phys. Chem. A., 101, 6922–6930, 1997.

Zhou, X., Beine, H. J., Honrath, R. E., Fuentes, J. D.: Simpson, W., Shepson, P. B., and Bottenheim, J.: Snowpack Photochemical Production as a Source for HONO in the Arctic Boundary Layer in Spring Time, Geophys. Res. Lett., 28, 21, 4087–4090, 2001.